



Modeling studies of tidal dynamics and the associated responses to coastline changes in the Bohai Sea, China

Longhai Zhu^{1,2} · Rijun Hu^{1,2} · Haijun Zhu³ · Shenghui Jiang^{1,2} · Yongchen Xu⁴ · Nan Wang⁴

Received: 3 November 2017 / Accepted: 2 August 2018 / Published online: 22 August 2018
© Springer-Verlag GmbH Germany, part of Springer Nature 2018

Abstract

Over the past 30 years, reclamation projects and related changes have impacted the hydrodynamics and sediment transport in the Bohai Sea. Three-dimensional tidal current models of the Bohai Sea and the Yellow Sea were constructed using the MIKE 3 model. We used a refined grid to simulate and analyze the effects of changes in coastline, depth, topography, reclamation, the Yellow River estuary, and coastal erosion on tidal systems, tide levels, tidal currents, residual currents, and tidal fluxes. The simulation results show that the relative change in the amplitude of the half-day tide is greater than that of the full-day tide. The changes in the tidal amplitudes of M_2 , S_2 , K_1 , and O_1 caused by coastline changes accounted for 27.76–99.07% of the overall change in amplitude from 1987 to 2016, and water depth changes accounted for 0.93–72.24% of the overall change. The dominant factor driving coastline changes is reclamation, accounting for 99.55–99.91% of the amplitude changes in tidal waves, followed by coastal erosion, accounting for 0.05–0.40% of the tidal wave amplitude changes. The contribution of changes in the Yellow River estuary to tidal wave amplitude changes is small, accounting for 0.01–0.12% of the amplitude change factor. The change in the highest tide level (HTL) is mainly related to the amplitude change, and the correlation with the phase change is small. The dominant factor responsible for the change in the HTL is the tide amplitude change in M_2 , followed by S_2 , whereas the influence of the K_1 and O_1 tides on the change in the HTL is small. Reclamation resulted in a decrease in the vertical average maximum flow velocity (V_{VAM}) in the Bohai Sea. Shallower water depths have led to an increase in the V_{VAM} ; deeper water depths have led to a decrease in the maximum flow velocity. The absolute value of the maximum flow velocity gradually decreases from the surface to the bottom, but the relative change value is basically constant. The changes in the tidal dynamics of the Bohai Sea are proportional to the degree of change in the coastline. The maximum and minimum changes in the tidal flux appear in Laizhou Bay (P-LZB) and Liaodong Bay (P-LDB), respectively. The changes in the tidal flux are related to the change in the area of the bay. Due to the reduced tidal flux, the water exchange capacity of the Bohai Sea has decreased, impacting the ecological environment of the Bohai Sea. Strictly controlling the scale of reclamation are important measures for reducing the decline in the water exchange capacity of the Bohai Sea and the deterioration of its ecological environment.

Keywords Bohai Sea · Coastline change · Tidal dynamics · Simulation · MIKE 3

Responsible Editor: Guoping Gao

✉ Rijun Hu
HRJ@ouc.edu.cn

¹ Key Lab of Submarine Geosciences and Prospecting Techniques.MOE, Qingdao 266100, China

² College of Marine Geosciences, Ocean University of China, No. 238, Songling Road, Qingdao 266100, Shandong, China

³ Key Laboratory of Marine Food Quality and Hazard Controlling Technology of Zhejiang Province, China Jiliang University, Hangzhou 310018, China

⁴ Ocean University of China, No. 238, Songling Road, Qingdao 266100, Shandong, China

1 Introduction

The coastal zone represents the interface between the land and sea, and frequent exchanges of material and energy occur among the climate system, groundwater systems, biosphere, soil, and sediment on land and in the sea in this zone (Gao et al. 2014). Tidal flats, the buffer zones between terrestrial and marine environments, are of substantial importance to the hydrodynamics, sedimentology, and ecosystems of adjacent estuaries, lagoons, bays, and basins (Gao et al. 2017). Consequently, the loss of tidal flats due to land reclamation has recently drawn special attention from many coastal scientists, engineers, and managers (Flemming and Nyandwi 1994; Gao et al. 2014; Li et al. 2014a, b; Nichols et al. 1986; Song

and Wang 2013). Coastal reclamation in China, which began in 1950 and was intended to accelerate economic development and alleviate the shortage of land resources, has caused nearly 50% of coastal wetlands to disappear (Gu et al. 2007). From 1985 to 2010, the coastal provinces and metropolises of China reclaimed 754,697 ha of coastal wetlands; after 2005, this process showed an increasing trend (Tian et al. 2016). The reclamation of near-sea areas results in an increase in the concentration of suspended solids in the sea (van Maren et al. 2016) and a significant reduction in benthic species and biomass (Yang et al. 2016). The impact of these changes on the benthic environment has a historically cumulative effect (Shen et al. 2016).

The unique natural environment of bays has caused bays to become increasingly important to modern society. Reclamation is an effective way to address shortages in land resources (Li et al. 2014a, b). However, as a result of the uncontrolled reclamation of bays, a number of environmental problems have arisen. For example, from 1968 to 1983, reclamation in Tokyo Bay caused the entrance flow velocity to decrease by 20%. Moreover, the tidal flux decreased by 35%, the abundance of beach mud increased, and other issues arose (Yanagi and Ohnishi 1999). By 1990, San Francisco Bay contained approximately 800 km² of reclaimed wetland and its water exchange capacity and tidal flux had decreased sharply, leading to a decline in biodiversity and deposition, as well as other issues (Parker et al. 1972; Takekawa et al. 2006). At present, the environmental problems caused by reclamation are gaining increased attention, and countries have taken a number of measures to protect their gulf environments (Li et al. 2014a, b).

The coastline, which represents the boundary between the land and the sea, is dynamic in nature. Identifying the location of the coast is critical in understanding the dynamic changes in coastal areas, especially those of the coastline (Pardo-Pascual et al. 2012). Coastlines undergo frequent short- and long-term changes that are caused by hydrodynamic changes (e.g., river cycles and sea-level rise), geomorphological changes (e.g., barrier island formation and spit development), and other factors (e.g., sudden and rapid seismic and storm events and anthropogenic activities) (Jabaloy-Sánchez et al. 2010).

The Bohai Sea (BHS) is a semi-enclosed sea in northern China that has been studied by many oceanographers from China and other countries (Fig. 1). The sea can be divided into four parts: Bohai Bay, Laizhou Bay, Liaodong Bay, and the central BHS (Jiang 2004). From the 1930s to the 1970s, the half-day tidal wave in the southern part of the BHS changed considerably due to changes in the coastline and water depth of the BHS (Huang 1991). The total coastline length in the BHS increased by 633.7 km at an average rate of 25.3 km/year. The total area of the BHS decreased by 1593.44 km² from 1987 to 2012 at an average rate of 63.7 km²/year (Zhu et al. 2014). The coastline of the Yellow River estuary has

extended outward toward the ocean, and the total length of the coastline has increased by approximately 298.8 km from 1973 to 2014 (Wang et al. 2016). The change in the coastline caused by reclamation has resulted in an increase of 0.1–0.2 m in the maximum tide of Bohai Bay. Considering the effects of storm surge, the total water level is close to or exceeds the warning level of the port in the bay (Ding and Wei 2017). Different researchers have analyzed the trends of the dynamic changes caused by the reclamation of local areas within the BHS and Bohai Bay (Jiang et al. 2015; Zhang and Wang 2000; Zhang et al. 2015). The mean sea level (MSL) has risen and the mean large tidal range (MLTR) has become larger because of sediment accumulation and subsidence in the areas around the Huanghe River mouth (Zhang and Wang 2000). There have indeed been significant changes in the tidal regime in the BHS from 1976 to 2011, with the amplitude of M2 changing by up to 20 cm in some areas (Pelling et al. 2013).

In previous research results, the emphasis was generally placed on the simulation of a single influencing factor, such as reclamation or changes in the Yellow River estuary or the simulation using the M2 tide. On the basis of this previous work, this paper adopted the fine-mesh in the numerical model, which enables to verify the impact of narrow structure such as the gigantic jetties extending from Hanghua and Weifang Ports not fully resolved in conventional models. Also, this paper used nine major tides to carry out a single-factor simulation of the tidal current dynamics under the influence of various factors, such as changes in the coastline of the BHS, changes in water depth, changes in the reclamation, changes in the Yellow River, and coastal erosion over the past 30 years. This paper fully considers coastline changes in the Liaodong Bay taken place mainly in 2010s, which is different from the paper of Pelling et al. (2013). Using this comprehensive simulation, the changes in the BHS wave system, tide levels, currents, residual currents, and tidal fluxes, as well as the correlations and relative contributions of various factors, were explored, and the factors controlling the tidal current dynamic changes in the BHS were revealed. The study is of great significance for further improving the research results of the interaction mechanisms between human activities and tidal dynamics.

The following steps were carried out as part of the study described in this paper. Satellite images were used to extract the coastlines corresponding to 1987 and 2016; three-dimensional flow models of the BHS were constructed; the model was verified; the flow fields of the BHS in 1987 and 2016 were simulated; and the changes in the tidal wave systems, tide levels, tidal currents, residual flows and tidal fluxes in the BHS from 1987 to 2016 were analyzed. Moreover, the results of this paper provide a basis for further studies of the transport of the BHS sediments.

The rest of the paper is organized as follows. The second section describes the source of the coastline data, the

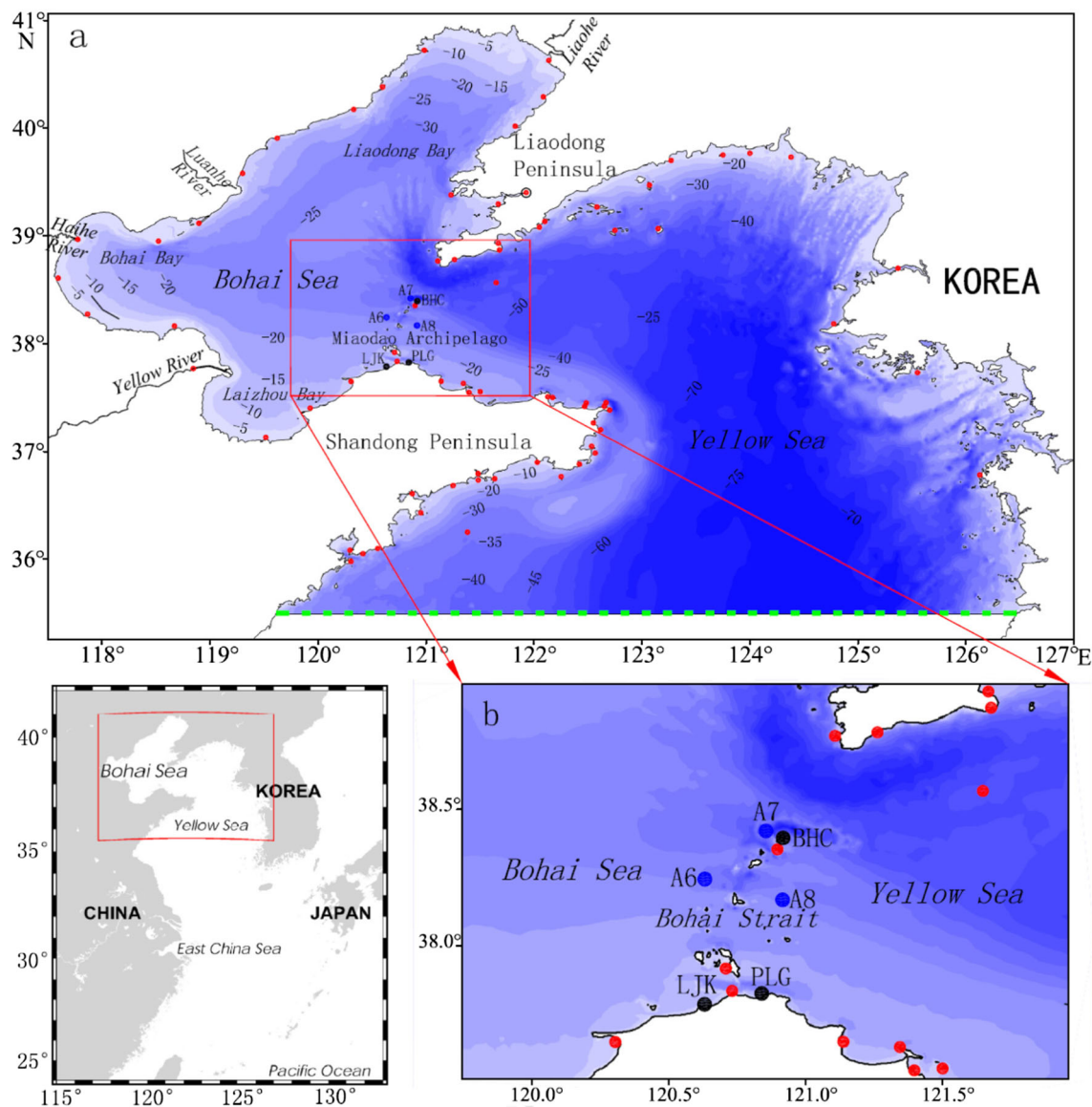


Fig. 1 Location of the study area. **a** Bathymetric map of the BHS in 1984 that shows the model domain. The dotted line indicates the boundary of the domain in the Yellow Sea. The red dots show the locations of

historical tidal gauges. **b** A6, A7, and A8 indicate the locations of tidal current stations. Beihuangcheng (BHC), Penglaigang (PLG), and Luanjiakou (LJK) are tidal elevation stations

distribution of water depths, the tide levels, and the trends in the data. The third section introduces the method of interpreting the coastline data, the numerical simulation method, and the model verification. The fourth section presents the simulation results, and the fifth section describes the conclusions.

2 Study site and data

2.1 Tidal environment of the BHS

The Bohai Sea, which is a semi-enclosed continental shelf in northern China, is located between the range 37° 07' N to 41°

N and the range 117° 35' E to 121° 10' E. It is surrounded by land on the north, west, and south sides and is connected to the Yellow Sea through the narrow Bohai Strait, which is approximately 90-km wide. The Bohai Sea is very shallow with depths less than 30 m in 95% of the area. The average water depth is only 18 m. The area with depth of more than 30 m is mainly located in the northern section of the Bohai Strait (Jiang et al. 2000). The Bohai Sea consists of five areas: the Liaodong Bay, the Bohai Bay, the Laizhou Bay, the Bohai Strait, and the central area (as shown in Fig. 1). The Yellow River is a major river in the study area.

The topography of the BHS is shown in Fig. 1. The M2 tide is the principal tidal component in the area. Two amphidromic points are located offshore of Qinhuangdao and the Yellow

(Huanghe) River estuary. The K1 tide has an amphidromic point at the southern part of the Bohai Strait (Editorial Board Marine Atlas 1994). Tidal ranges greater than 3.5 m have been observed at the head of the Liaodong Bay, and the maximum possible tidal current was calculated to be greater than 120 cm/s in the Bohai Strait (Xiong 2012).

2.2 Coastline data

The coastline is the most basic information needed for ocean tide and tidal current modeling. The coastline was derived from satellite data. In total, 14 scenes of Landsat TM and OLI_TIRS remote sensing data collected at multiple points between 1987 and 2016 (the detailed acquisition dates are provided in Table 1, numbers 1 to 14) were employed in this research. The data were processed using GIS techniques. The spatial resolutions of the TM and OLI_TIRS data are 30 and 15 m, respectively.

The method of White and El Asmar (1999) was employed in this paper. Using second-order polynomials, the Landsat images were registered to geographical coordinates to transform the line and column locations of the pixels to their corresponding latitudinal and longitudinal locations. A 1:50,000 topographic map was used as a reference to rectify these images. Control points were selected from the remote sensing images for alignment with the corresponding locations in the 1:50,000 topographic map in the geo-referencing process.

2.3 Topographic data

High-precision water depth data are critical for offshore numerical modeling. The research team has conducted years of research in the BHS, collecting a large amount of high-

precision water depth terrain data. To set up the models for 1987 and 2016, the team collected the bathymetric data covering the area off of BHS from sea charts published by the Navigation Guarantee Department of the Chinese Navy Headquarters and the China Maritime Safety Administration between 1984 and 1994 and between 2007 and 2014, respectively. To be consistent with the analysis of the changes in the coastline, the results are referred to as the water depth in 1987 (as shown in Fig. 2a) and the water depth in 2016 (as shown in Fig. 2b). From 1987 to 2016, the water depth has undergone major changes. Maximum deposition occurred on the southeastern side of the Yellow River, reaching a thickness of 12.4 m, and erosion occurred in the southern part of Bohai Bay. The maximum amount of erosion was 5.6 m (as shown in Fig. 2c). As changes in the coastline may affect the nearshore water depths, some of the water depth data have been corrected.

2.4 Verification data

Measured tide level and tidal current data are very important for verifying the model results. To validate the tidal model for 1987, we collected data from 65 stations with historical tidal observations. To validate the tidal model for 2016, we collected data from 54 stations with historical tidal observations, used the tidal elevation data from the Beihuangchen (BHC), Penglaigang (PLG), and Luanjiakou (LJK) stations (Fig. 1b) and the tidal current data from three stations (A6–A8) in the mouth of the BHS (Fig. 1b). These in situ data were obtained from field surveys conducted by the Ocean University of China. The tidal elevations were collected by tidal gauges located at BHC, PLG, and LJK. The tidal elevation data cover the period from August 3 to 18, 2016, and were collected at 2-

Table 1 List of different satellite data

| Number | Acquisition date | Satellite | Sensor | Path/row | Bands | Spatial resolution (m) |
|--------|------------------|-----------|----------|----------|-------|------------------------|
| 1 | 1987.6.24 | Landsat5 | TM | 121/33 | 7 | 30 |
| 2 | 2016.8.26 | Landsat8 | OLI_TIRS | 121/33 | 8 | 15 |
| 3 | 1987.6.15 | Landsat5 | TM | 122/33 | 7 | 30 |
| 4 | 2016.5.13 | Landsat8 | OLI_TIRS | 122/33 | 8 | 15 |
| 5 | 1987.6.24 | Landsat5 | TM | 121/34 | 7 | 30 |
| 6 | 2016.8.26 | Landsat8 | OLI_TIRS | 121/34 | 8 | 15 |
| 7 | 1987.9.21 | Landsat5 | TM | 120/34 | 7 | 30 |
| 8 | 2016.7.2 | Landsat8 | OLI_TIRS | 120/34 | 8 | 15 |
| 9 | 1987.9.21 | Landsat5 | TM | 120/33 | 7 | 30 |
| 10 | 2016.6.16 | Landsat8 | OLI_TIRS | 120/33 | 8 | 15 |
| 11 | 1987.9.21 | Landsat5 | TM | 120/32 | 7 | 30 |
| 12 | 2016.7.2 | Landsat8 | OLI_TIRS | 120/32 | 8 | 15 |
| 13 | 1987.6.24 | Landsat5 | TM | 121/32 | 7 | 30 |
| 14 | 2016.8.26 | Landsat8 | OLI_TIRS | 121/32 | 8 | 15 |

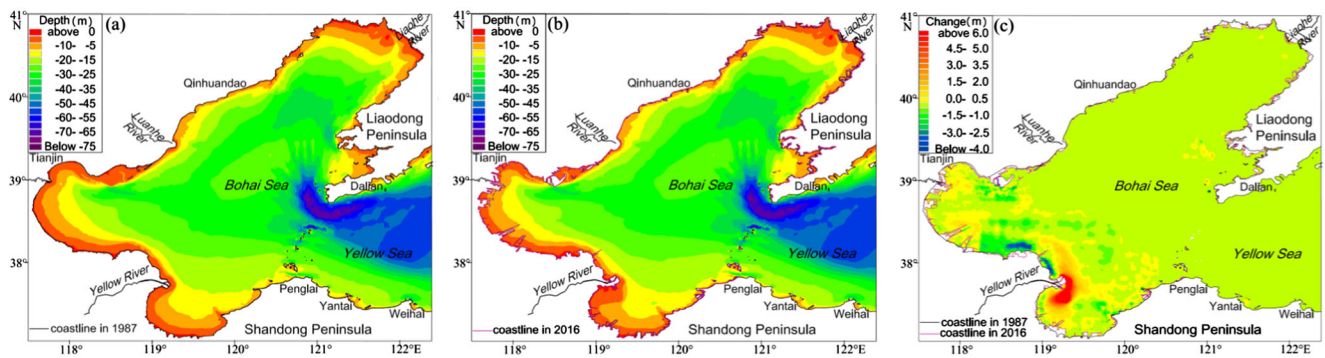


Fig. 2 Topography and changes in water depth. **a** The water depth of the Bohai Sea in 1987. **b** The water depth of the Bohai Sea in 2016. **c** The difference in water depth between 2016 and 1987

min intervals. A FlowQuest 600 ADCP was used to record the speeds and directions of the tidal currents. The tidal currents were observed at 10-min intervals during a spring tide (9:00 a.m. August 3 to 12:00 a.m. August 4, 2016).

3 Methodology

3.1 Coastline interpretation

The average high tide line, which represents the coastline, was manually delineated by a single person, relying on their knowledge of the morphological features; vegetation; and sedimentary characteristics (color, sediment type, and water content). This procedure was carried out at a single scale to ensure high accuracy for each combined TM 432 pseudo-color image. The mean high tide line is a better representation than the water/land line, which is easily affected by sea ice and tides (Chu et al. 2006).

Where seawalls, salt ponds, culture ponds, or reclamation areas exist along the coast, the seawall was treated as the coastline. The coastline vector maps, which were extracted from satellite images, show that the coastline of the BHS changed considerably from 1987 to 2012 (Fig. 3, Table 2). These changes are especially notable in areas including the Yellow River Delta, Caofeidian, the Tianjin and Huanhuang ports of Bohai Bay, and the Weifang Port of Laizhou Bay. The areas of changes in the reclamation, changes in the Yellow River, and coastal erosion are shown in Table 3.

3.2 Numerical model

3.2.1 Model description

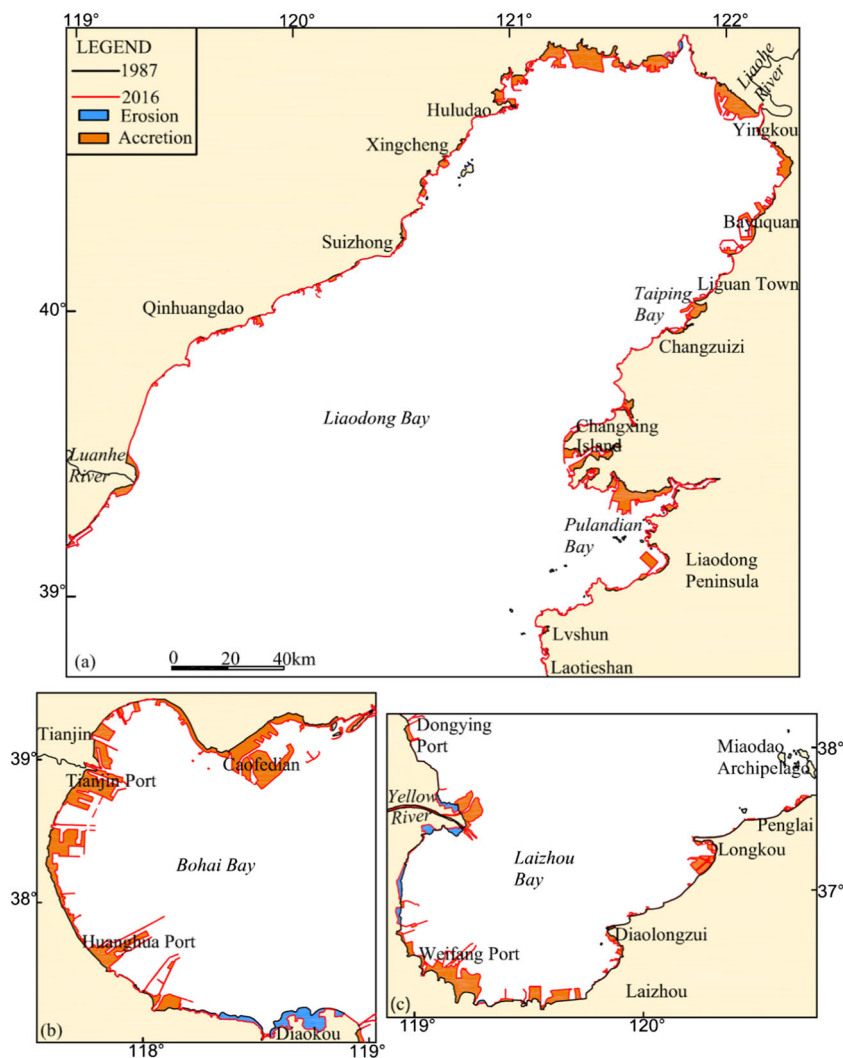
The simulations presented herein were performed using the commercially available MIKE 3 Flow Model FM (flexible mesh). The momentum equations used are the incompressible, Reynolds-averaged form of the Navier–Stokes equations (RANS), invoking the Boussinesq assumption and the

hypothesis of vertical hydrostatic pressure. The turbulence closure is achieved using the Smagorinsky formulation for the horizontal diffusion, and the standard k – ϵ model is used to represent diffusion in the vertical direction. To account for the Coriolis force, an f -plane has been used. The free surface is taken into account using a sigma-coordinate transform. The spatial discretization of the primitive equations is performed using a cell-centered finite volume method. In the horizontal plane, an unstructured grid was used, while the discretization is structured in the vertical direction (Danish Hydraulic Institute 2016). The temperature and salinity structure has obvious seasonal characteristics in the BHS (Liu et al. 2003). There is no apparent vertical structure of the temperature and salinity in autumn, winter, and spring. In summer, temperature stratification occurs in the BHS (Xiong 2012). Since the average depth of the BHS is only 18 m, wave action induces relatively homogenous mixing of the seawater (Hu et al. 2004). Over the past 50 years, due to natural factors and artificial dam construction, the amount of sediment entering the Yellow River has been dramatically reduced (Wang et al. 2006, 2007). Low-salinity conditions appear mainly in local areas near the estuary during flood seasons. In these areas, the salinity distribution is more uniform at other times. Therefore, this paper uses a barotropic flow numerical model that does not consider changes of temperature and pressure.

3.2.2 Model domain

The simulation domain covers the entire BHS, including parts of the adjacent Yellow Sea (Fig. 1a). The mesh is fine at the mouth of the bay and in the nearshore zone, where it has a minimum grid size of 55 m, but it is coarser in the middle part of the inner bay and over the open sea, with a maximum grid size of 8262 m (Fig. 4). The numbers of model elements and nodes present within the whole model domain in 1987 are 196,173 and 106,103, respectively. The numbers of model elements and nodes present within the whole model domain in 2016 are 179,869 and 99,897, respectively. As this study focuses on barotropic hydrodynamics, 11 vertical layers are used. The thickness of the surface and bottom layers is 0.05

Fig. 3 Changes in the coastline of the BHS from 1987 to 2016 in **a** Liaodong Bay, **b** Bohai Bay, and **c** Laizhou Bay



times the water depth; the thickness of the other nine layers is 0.10 times the water depth.

Due to the existence of a large area of intertidal zone in Bohai Sea, especially in Laizhou Bay, in order to reflect the impact of intertidal zones change, the statistical results of tidal levels in different regions were collected to determine the mean high tide level in different regions as the water depth of the upper part of the intertidal zone. Then, the water depth of different parts of the tidal flat is obtained by interpolating the water depth of the high tide line and the depth of the chart.

3.2.3 Initial and boundary conditions

The oceanic open boundary is located outside the BHS and extends into the Yellow Sea. The open boundary conditions for the water level were specified using the tidal elevations predicted by the nine major tidal constituents (M_2 , S_2 , K_1 , O_1 , Q_1 , P_1 , N_2 , K_2 , and Sa) (Qian and Sheng 2000). Numerous rivers flow into the BHS, and the Yellow River is famous for its high concentration of sediments. The average runoff of the

Yellow River is $49 \times 10^9 \text{ m}^3/\text{year}$, and the annual sediment discharge is 1.1×10^9 tons (Ren and Shi 1986). The sediment and water discharges of the Yellow River display strong seasonal variations. The majority of the water and sediment discharges occur during the flood season (July to September). In the BHS, wave heights and wave directions differ seasonally. Thus, river runoff and waves were not taken into account by studies focusing on the tidal dynamics of the BHS. The thermal stratification and surface wind forces should be included in future models. The models used constant values of salinity (30.3 psu) and temperature ($25.3 \text{ }^\circ\text{C}$) based on the mean salinity and temperature values during the summer season (Liu et al. 2003).

3.2.4 Model experiments

To study the influence of coastline changes on tidal power over the past 30 years, seven sets of simulation experiments were conducted (see Table 4 for details). Run1 involves the coastline of 1987 and the water depth from 1984 to 1994

Table 2 Changes in the coastline length and area of the BHS

| Bay | 1987 | | 2016 | | Difference/percentage change | |
|--------------|-------------------------|-----------------------|-------------------------|-----------------------|------------------------------|---------------------------|
| | Area (km ²) | Coastline length (km) | Area (km ²) | Coastline length (km) | Area (km ²)/(%) | Coastline length (km)/(%) |
| Laizhou Bay | 10,096.58 | 443.06 | 9741.51 | 902.92 | − 355.07/3.5 | 459.86/103.8 |
| Bohai Bay | 12,381.85 | 451.93 | 11,755.13 | 1137.58 | − 626.72/5.1 | 685.65/151.7 |
| Liaodong Bay | 34,864.61 | 1333.25 | 33,956.90 | 1859.90 | − 907.71/2.6 | 526.65/39.5 |
| Bohai Sea | 77,082.01 | 2364.61 | 75,192.50 | 4036.77 | − 1889.51/2.5 | 1672.16/70.7 |

(referred to as the water depth in 1987), and the scheme is abbreviated Run1 (1987). Run2 involves the coastline of 2016 and the water depth from 2007 to 2014 (referred to as the water depth in 2016), and this scheme is called Run2 (2016). Run3 simulate the tidal dynamics after the water depth changes. The sea was converted to land in some area especially around the Yellow River estuary from 1987 to 2016. In order to ensure that seawater does not enter these lands during highest tide, the elevation of these areas is set to 10 m above mean sea level. Run4 simulate the tidal dynamics after the coastline changes. Run5 to Run7 simulate the tidal dynamics after the coastal line changes caused by changes in the reclamation of the sea, the Yellow River, and coastal erosion.

3.2.5 Model validation

Model validation is vital to this paper. The MIKE 21 tidal analysis program was used to extract the main tidal constituents from the modeled tidal elevations. The tidal amplitudes and phases derived from the model run for 1987 and 2016 agreed well with those recorded at the historical tidal observation stations (Figs. 5, 6). First, the difference between the simulated harmonic constants (amplitude and phase) and observed harmonic constants for each station was calculated. Then, take the difference as an absolute value ($|Amplitude_{simulated} - Amplitude_{observed}|$, $|Phase_{simulated} - Phase_{observed}|$), and convert all the differences into positive value. Finally, the average value of the absolute difference between the simulated and observed amplitude and the average value of the phase absolute difference of all stations are calculated. The average value was called mean absolute error (MAE). The MAE between the simulated and observed M₂ amplitudes and phases for 1987 were 5.4 cm and 5.6°,

respectively, whereas the MAE between the simulated and observed K₁ amplitudes and phases for 1987 were 2.8 cm and 4.3°, respectively (Fig. 5). The MAE between the simulated and observed M₂ amplitudes and phases for 2016 were 5.8 cm and 6.0°, respectively, whereas the MAE between the simulated and observed K₁ amplitudes and phases for 2016 were 3.0 cm and 4.8°, respectively (Fig. 6).

Data from BHC, PLG, and LJK from 2016 (Fig. 1b) were used to verify the modeled tide levels in 2016, and the observational data extends from August 3 to 18, 2016. Fig. 7 implies that the model results match the observational data well. The average absolute errors are 10.0, 8.4, and 6.4 cm at stations BHC, PLG, and LJK, respectively.

To verify the modeled flow velocities and flow directions, data collected at A6, A7, and A8 at 10-min intervals from August 3 to 4, 2016 (Fig. 1b), were used Fig. 8 implies that the model results and the observational data generally agree well. This verification of the model results has demonstrated the reliability of the model; thus, the model can be used for further simulations.

4 Model results

Based on the reliability analysis of the model, we have adopted a single-factor simulation and a comprehensive simulation of the tidal current dynamics under the influence of various factors, such as coastline changes, water depth changes, reclamation of the sea, changes in the Yellow River estuary, and coastal erosion, in the BHS over the past 30 years. The influence of these factors on the tidal wave system, tide level, tidal current, residual current, and tidal flux was analyzed.

Table 3 Changes in the area of the BHS caused by different factors

| Factor | Area in 1987 (km ²) | Area in 2016 (km ²) | Difference (km ²) | Percentage change (%) |
|-----------------------------|---------------------------------|---------------------------------|-------------------------------|-----------------------|
| Total coastline change | 77,082.01 | 75,192.5 | − 1889.51 | − 2.5 |
| Reclamation change | 77,082.01 | 75,362.87 | − 1719.14 | − 2.2 |
| Yellow River estuary change | 77,082.01 | 76,995.52 | − 86.49 | − 0.1 |
| Erosion change | 77,082.01 | 77,338.87 | 256.86 | 0.3 |



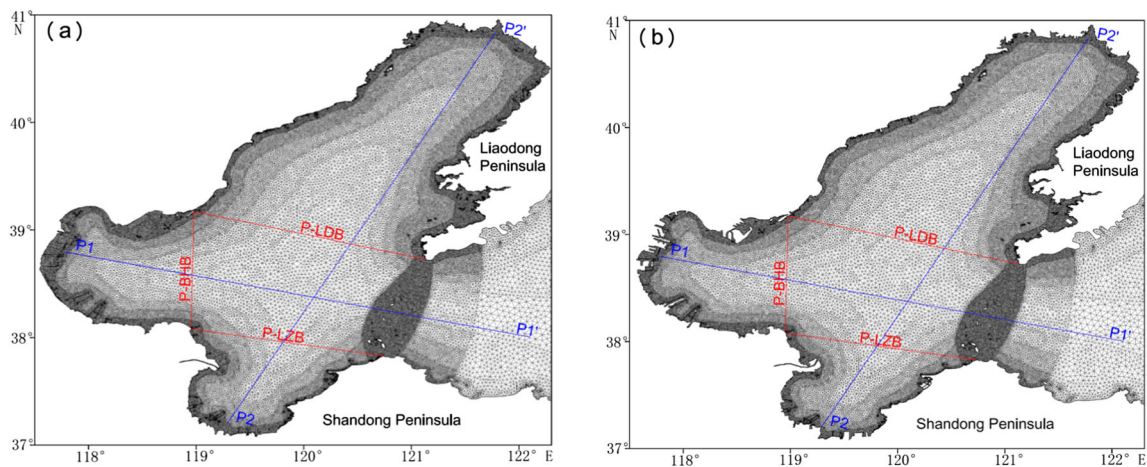


Fig. 4 Mesh and grid distribution in the BHS. **a** Mesh and grid distribution for 1987. **b** Mesh and grid distribution for 2016. In this figure, P-LZB, P-BHB, and P-LDB represent the profiles of the

Laizhou Bay mouth, the Bohai Bay mouth, and the Liaodong Bay mouth, respectively. P1-P1' and P2-P2' represent two typical sections

4.1 Tidal wave and tidal elevation

4.1.1 Tidal wave

The BHS is mainly affected by four tidal waves: M_2 , S_2 , K_1 , and O_1 (Huang 1991). Of these, the M_2 tide is the main tide in the BHS (Wang et al. 1999). To analyze the changes in the tidal wave system, we conducted a 2-month (1500 h) tidal simulation from July 20, 2016 to September 20, 2016. Then, we selected 721 h (1-h interval) of tidal level data (from 12:00 August 21, 2016 to 12:00 September 20, 2016) for the tide analysis of heights. The analysis tool is Tide Analysis of Height in Mike21 Toolbox. The tidal

harmonic analysis yields the amplitudes and phase of M_2 , S_2 , K_1 , and O_1 at each grid node in the simulation area. As the M_2 and S_2 tides are half-day tides, their variation patterns are similar, and the amplitude of the M_2 tide is much greater than that of the S_2 tide. The K_1 and O_1 tides are full-day tides, and their variation patterns are similar, although the K_1 tidal amplitude is much greater than that of O_1 . Therefore, the M_2 tide and the K_1 tide were chosen for further analysis in this study.

The simulation results show that the BHS half-day tidal wave experienced considerable changes from 1987 to 2016. The M_2 tidal amplitude has changed by -0.233 – 0.172 m. The change in the daily tidal wave is small, and the change in the

Table 4 Details of the model runs

| Run | Tidal forcing | Depth (year) | Coastline | Directions | Run name | Comparative analysis |
|-----|---------------|----------------------------------|-----------------------------------|---|--------------------|--------------------------------|
| 1 | 9 tides | 1984–1994 (called depth in 1987) | 1987 | Original | Run1 (1987) | |
| 2 | 9 tides | 2007–2014 (called depth in 2016) | 2016 | Considers all coastline and depth changes | Run2 (2016) | Run2-Run1 (total change) |
| 3 | 9 tides | 2007–2014 (2016) | 1987 | Considers depth changes, not coastline changes | Run3 (depth) | Run3-Run1 (depth change) |
| 4 | 9 tides | 1984–1994 (1987) | 2016 | Considers all coastline changes, not depth changes | Run4 (coastline) | Run4-Run1 (coastline change) |
| 5 | 9 tides | 1984–1994 (1987) | Reclamation coastline | Considers coastline changes caused by reclamation from 1987 to 2016, not depth changes | Run5 (reclamation) | Run5-Run1 (reclamation change) |
| 6 | 9 tides | 1984–1994 (1987) | Coastline of Yellow River estuary | Considers coastline changes caused by Yellow River estuary changes from 1987 to 2016, not depth changes | Run6 (estuary) | Run6-Run1 (estuary change) |
| 7 | 9 tides | 1984–1994 (1987) | Erosion coastline | Considers coastline changes caused by erosion from 1987 to 2016, not depth changes | Run7 (erosion) | Run7-Run1 (erosion change) |

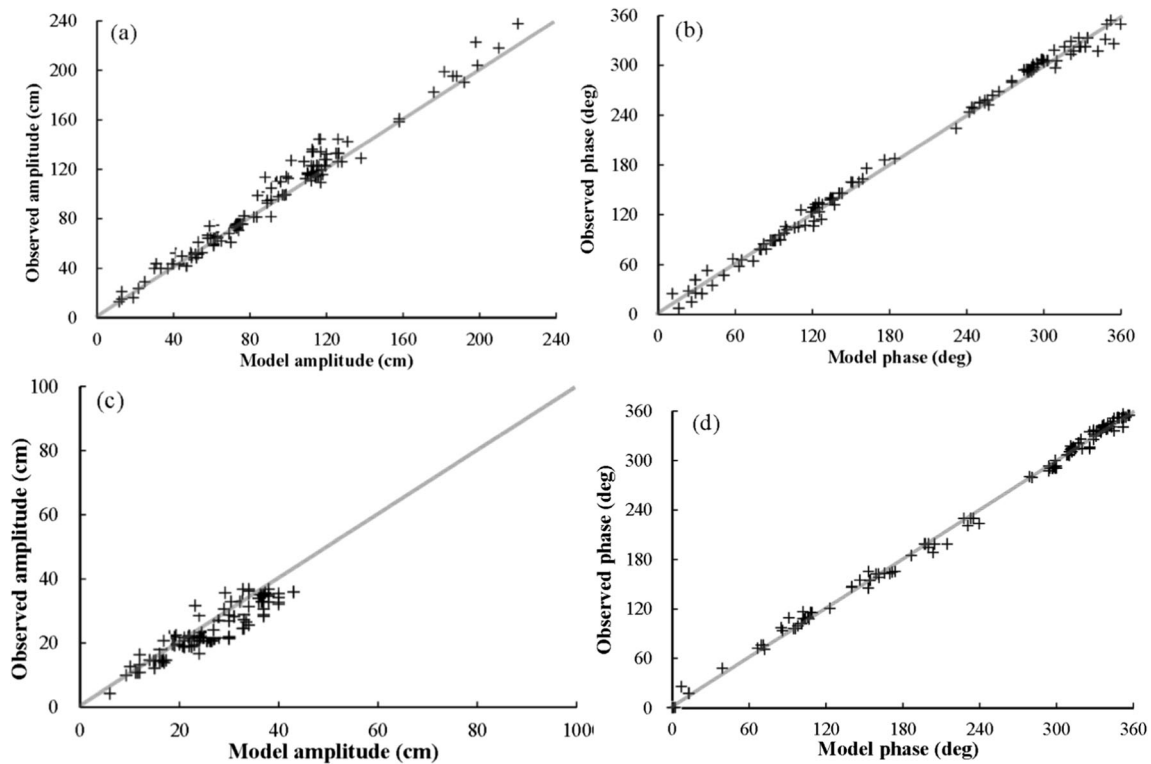


Fig. 5 Comparison of the observed data and the model results for 1987. **a** M₂ amplitude. **b** M₂ phase. **c** K₁ amplitude. **d** K₁ phase

K1 tidal amplitude is between -0.009 and 0.031 m. The Bohai M₂ amphidromic points and the K₁ amphidromic points appear to have migrated (Fig. 9b, d). For M₂, the amphidromic point in southern Qinhuangdao migrated

8.4 km southwest, and the amphidromic point in the northern Yellow River estuary migrated 16.7 km southeast. The amphidromic point of K₁ in the middle of the Bohai Strait migrated 4.6 km eastward.

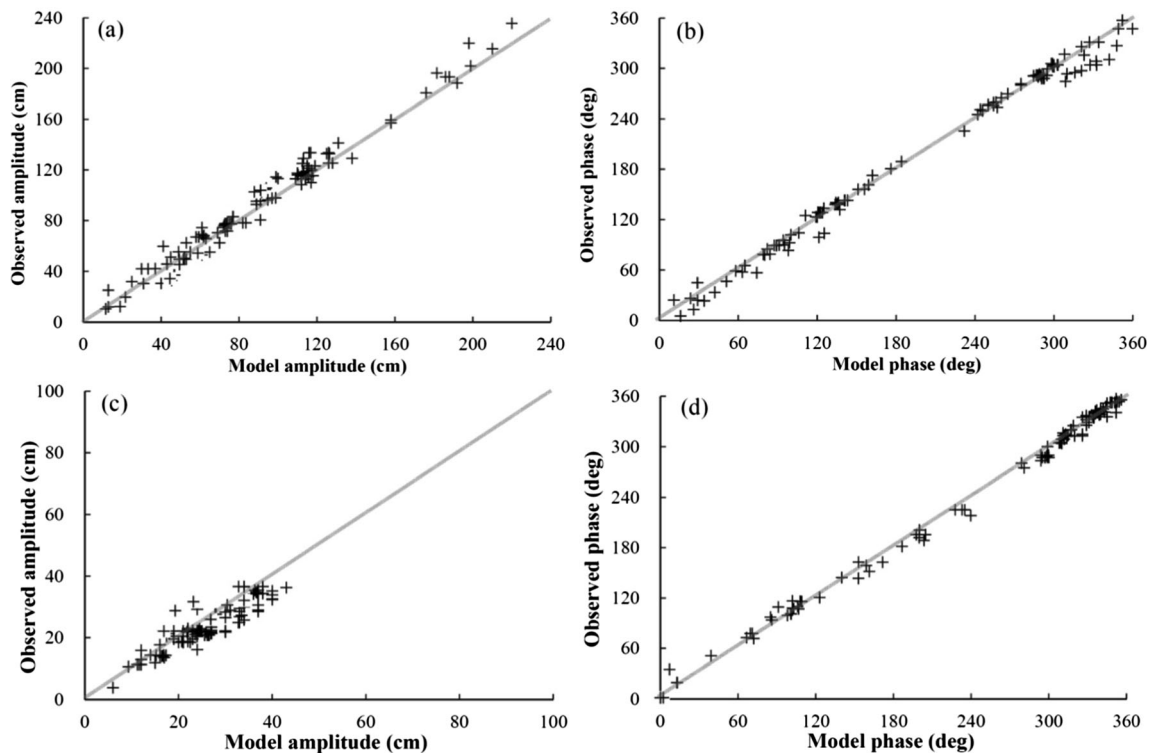


Fig. 6 Comparison of the observed data and the model results for 2016. **a** M₂ amplitude, **b** M₂ phase. **c** K₁ amplitude. **d** K₁ phase

To the south of the amphidromic point near Qinhuangdao and to the east of the amphidromic point near the Yellow River estuary, the BHS M₂ tidal amplitude decreased. The maximum amplitude reduction is 0.233 m. The M₂ tidal amplitudes increased to the north of the amphidromic point near Qinhuangdao and to the west of the amphidromic point near the Yellow River estuary (Fig. 9e). The amplitude of M₂ increased by up to 0.172 m. With the migration of the amphidromic points of M₂, the phase changed considerably near its two amphidromic points, with a maximum change of 177.8°. The tide levels changed considerably in different areas of the BHS. The amplitudes of Laizhou and Bohai Bays changed greatly, with maximum variations of 0.23 and 0.17 m, respectively. The amplitude changed slightly in Liaodong Bay, with a maximum change of 0.10 m. The amplitude changes of the Bohai Strait and the Yellow Sea were small, with maximum changes of 0.04 and 0.03 m, respectively.

Relative amplitude change and proportion of the BHS area is logarithmic relationship, but exhibit asymmetric features (as shown in Fig. 10). Because of the different factors, the amplitude of a part of the area increases, while the area of the other part decreases, but the area is not the same. For example, from 1987 to 2016, the area of M₂ and S₂ amplitude reduction area is much larger than that of the amplitude increase in the Bohai Sea (as shown in Fig. 10a). The change in water depth causes the area where the half-day tidal amplitude of the Bohai Sea to decrease is much larger

Fig. 7 Comparison of the modeled (dots) and observed (lines) tidal elevations at the BHC (a), PLG (b), and LJK (c) stations in 2016

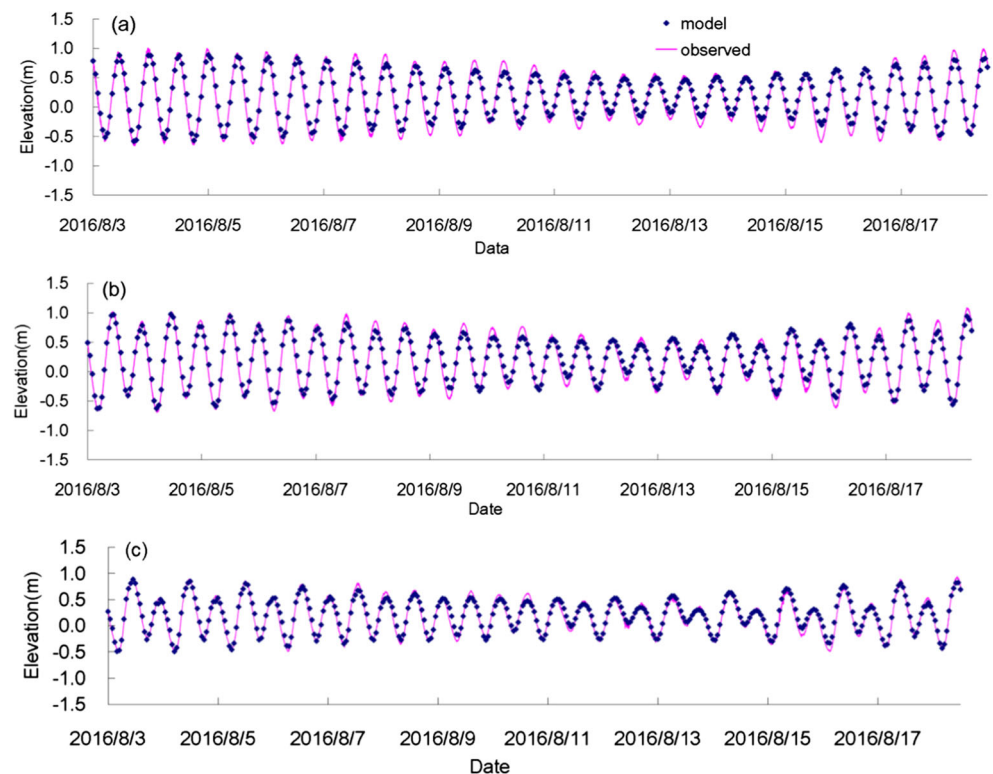
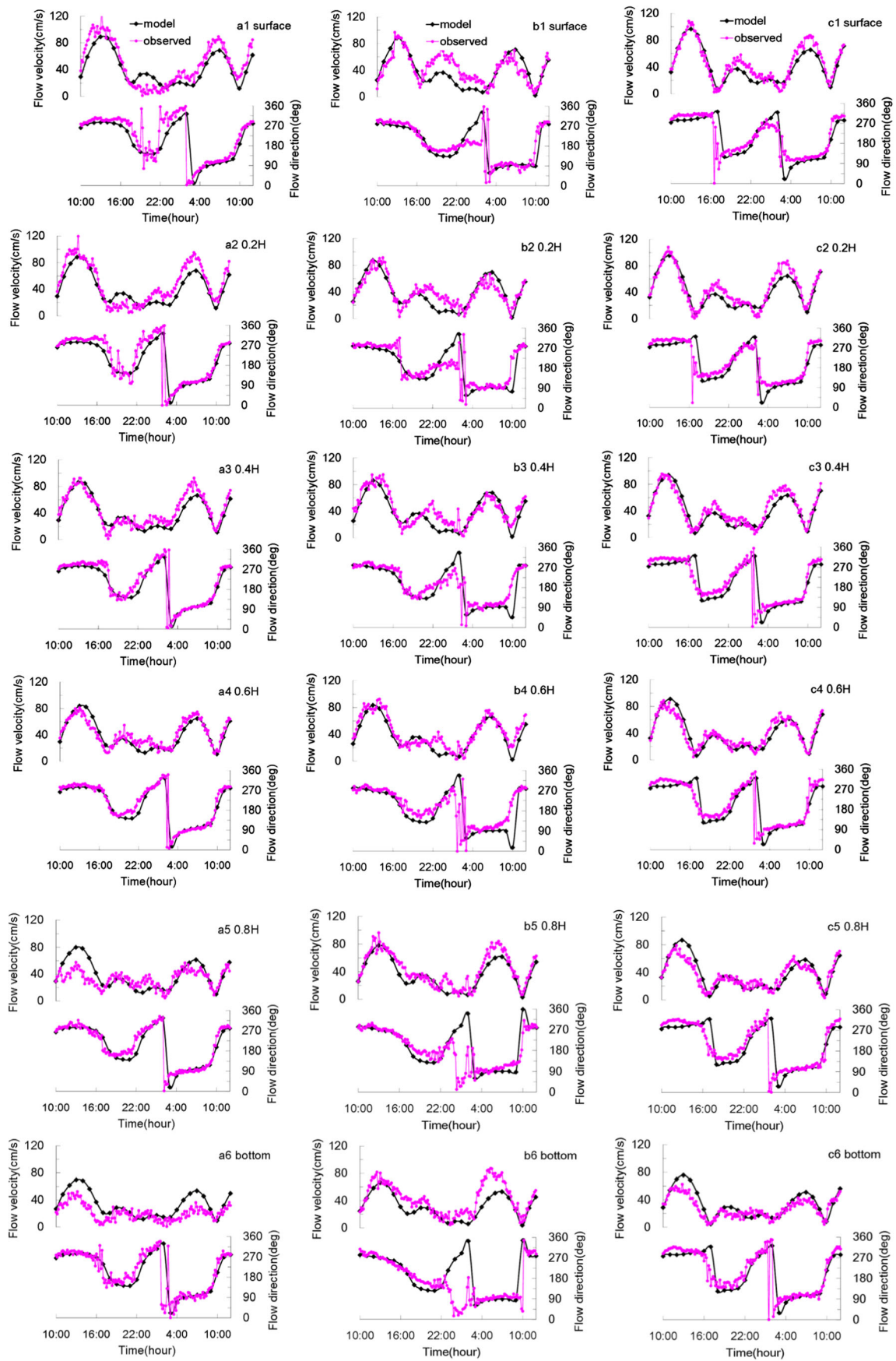


Fig. 8 Comparison of the modeled (black dotted line) and observed (pink dotted lines) flow velocities and directions from August 3 to 4, 2016. **a1–a6** Flow velocity and flow direction of the surface layer, 0.2 H (H is the water depth), 0.4 H, 0.6 H, and the bottom layer at station 6. **b1–b6** Flow velocity and flow direction at station 7. **c1–c6** Flow velocity and flow direction at station 8

than the area where the amplitude increases (as shown in Fig. 10b). The area where the M₂ tidal amplitude decreases is larger than the area where the amplitude increases, and the area of the S₂ amplitude increases is larger than the area of the amplitude decreases (as shown in Fig. 10d). The relative changes in the amplitudes of the half-day tides (M₂ and S₂) are basically the same. Additionally, the relative changes in the amplitudes of the full-day tides (K₁ and O₁) are also basically the same. However, the relative changes in the half-day tidal amplitudes are greater than those in the full-day tidal amplitudes. For example, the area where the M₂ amplitude is reduced by 5–10% accounts for 8.45% of the Bohai Sea area, while the area where the K₁ amplitude decreases by 5–10% only accounts for 0.76% of the Bohai Sea area (as shown in Fig. 10a) (as shown in Fig. 10a).

4.1.2 Tidal elevation

Because a single tidal amplitude cannot objectively reflect the highest tidal level of the sea, in this paper, we selected nine tidal waves for simulation, and selected tidal level data for a period of 1 month (721 h, 1-h interval) to extract the highest



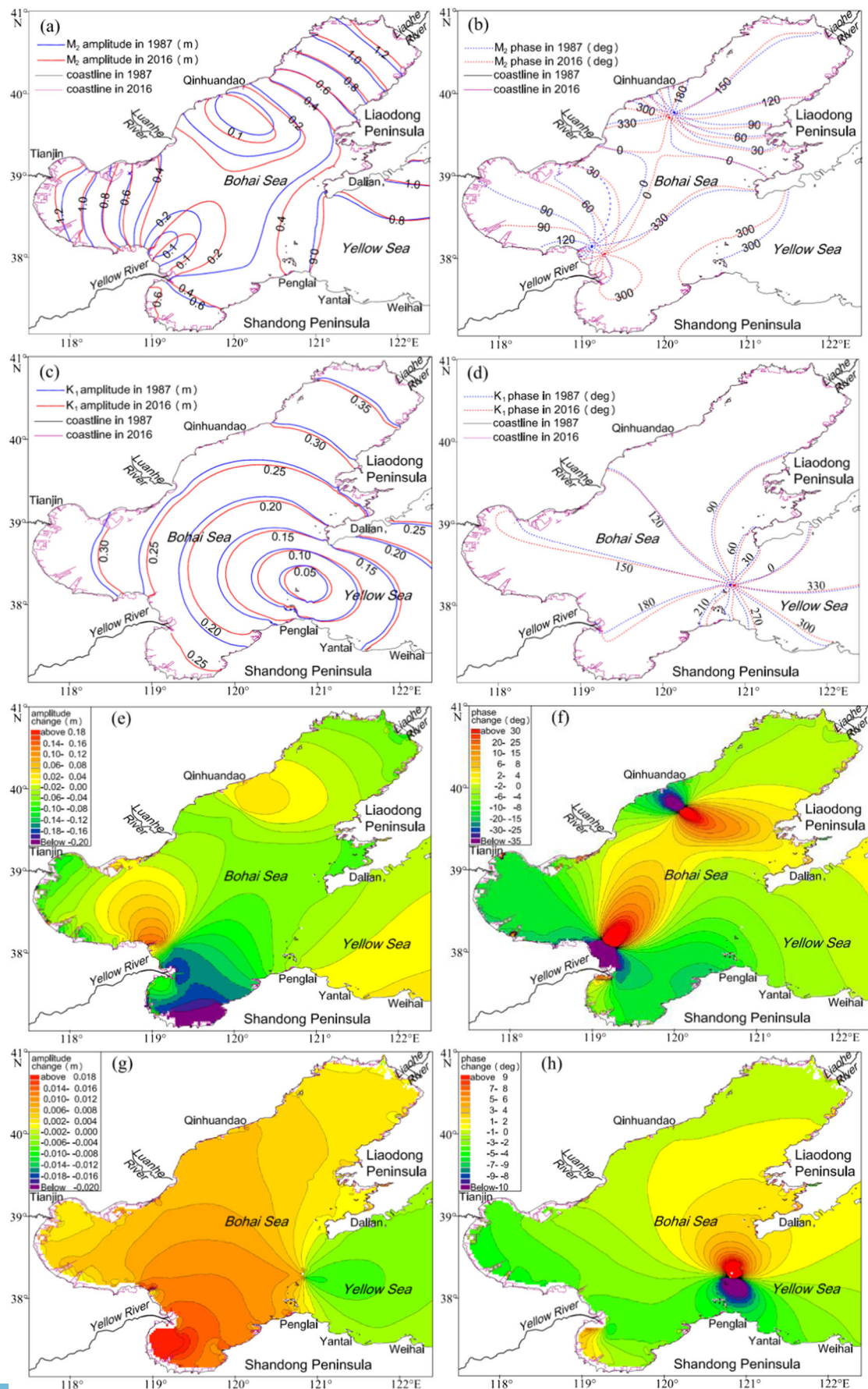


Fig. 9 Changes in tidal amplitudes and phases between 1987 and 2016 (M2 and K1). **a, b** M₂ tidal amplitudes and phases in 1987 and 2016. **c, d** K₁ tidal amplitudes and phases in 1987 and 2016. **e, f** Differences in the M₂ tidal amplitudes and phases between 1987 and 2016. **g, h** Differences in the K₁ tidal amplitudes and phases between 1987 and 2016

value of tidal level in each grid node as the highest tidal level (HTL). The highest tide level is an important basis for engineering design such as port terminal and coastal protection engineering. The change of the highest tide level has an important impact on the safety of offshore engineering. Therefore, research on the highest tide level changes is necessary. The following is a detailed analysis of the changes in the HTL in the Bohai Sea, results as shown in Fig. 11.

The simulation results show that the HTL in the BHS varied from -0.32 to 0.21 m between 1987 and 2016. The tide in Laizhou Bay showed a decreasing tendency, with the maximum reduction value of -0.32 m. The maximum tide levels in the Bohai and Liaodong Bays showed increasing trends at the

bay mouths or central and decreasing trends at the heads of the bays. The largest increase was 0.21 m (as shown in Fig. 11a). Changes in coastline and water depth have opposite effects on the maximum tide level. The change in coastline here refers to an increase in the length of the coastline of the Bohai Sea and a corresponding reduction in the area of the sea. The changes in the coastline led to an overall increase in the maximum tide levels in the Bohai and Liaodong Bays, with a maximum increase of 0.19 m, whereas the HTL in the Laizhou Bay showed a decreasing trend, with a maximum decrease of 0.43 m. The change in water depth led to a decreasing trend in the HTL in the BHS. The maximum reduction value was 0.24 m. The HTL in the southern Yellow River estuary increased by 0.25 m. Comparison of the P1-P1' section and the P2-P2' section reveals that the change in the HTL caused by the reclamation is basically consistent with the change caused by the coastline change. Therefore, reclamation is the main factor affecting the change in the HTL of the coastline.

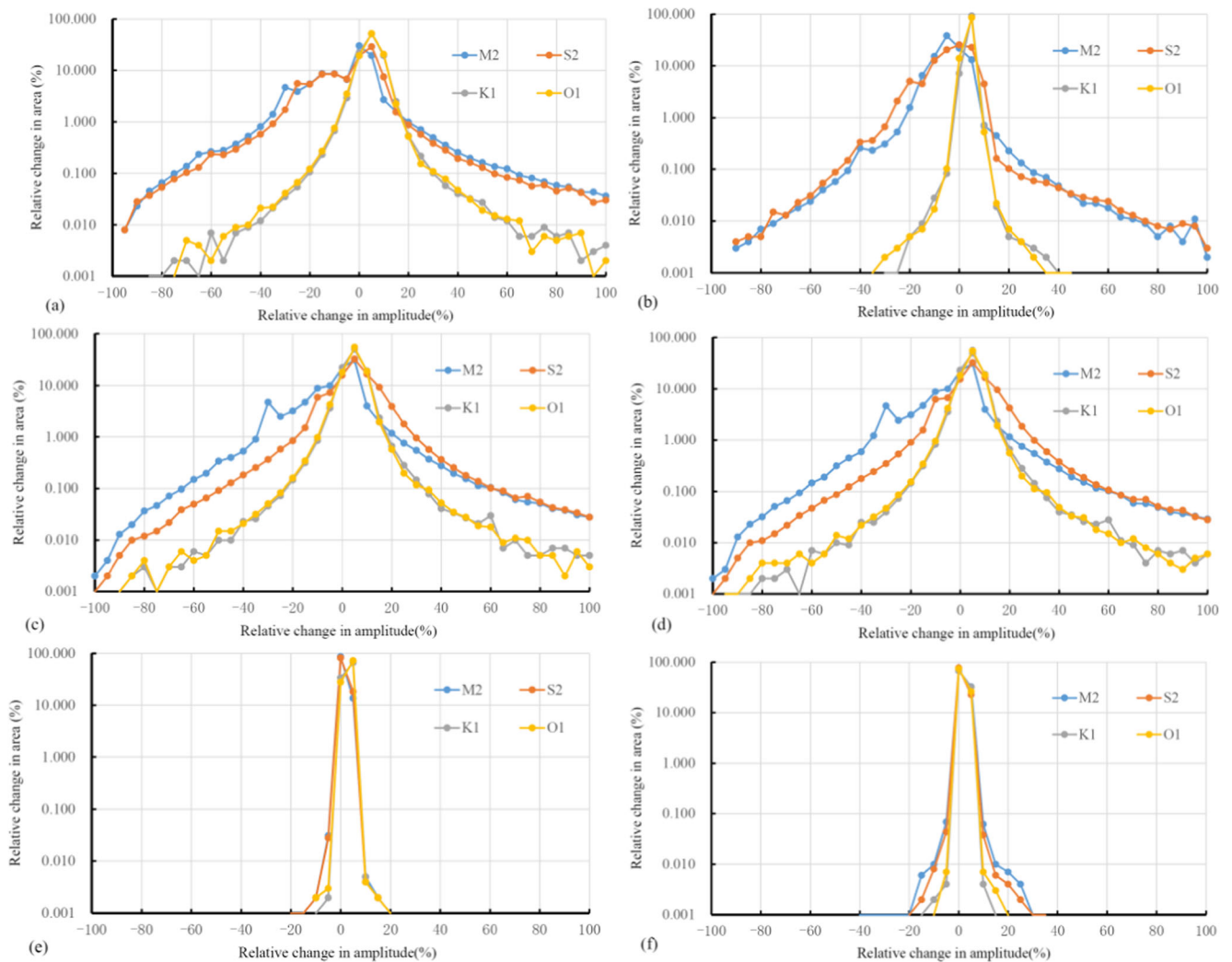


Fig. 10 Curves of relative tidal amplitude changes and the corresponding area. **a** Run2-Run1 (total change). **b** Run3-Run1 (depth change). **c** Run4-Run1 (coastline change). **d** Run5-Run1 (reclamation change). **e** Run6-Run1 (estuary change). **f** Run7-Run1 (erosion change)

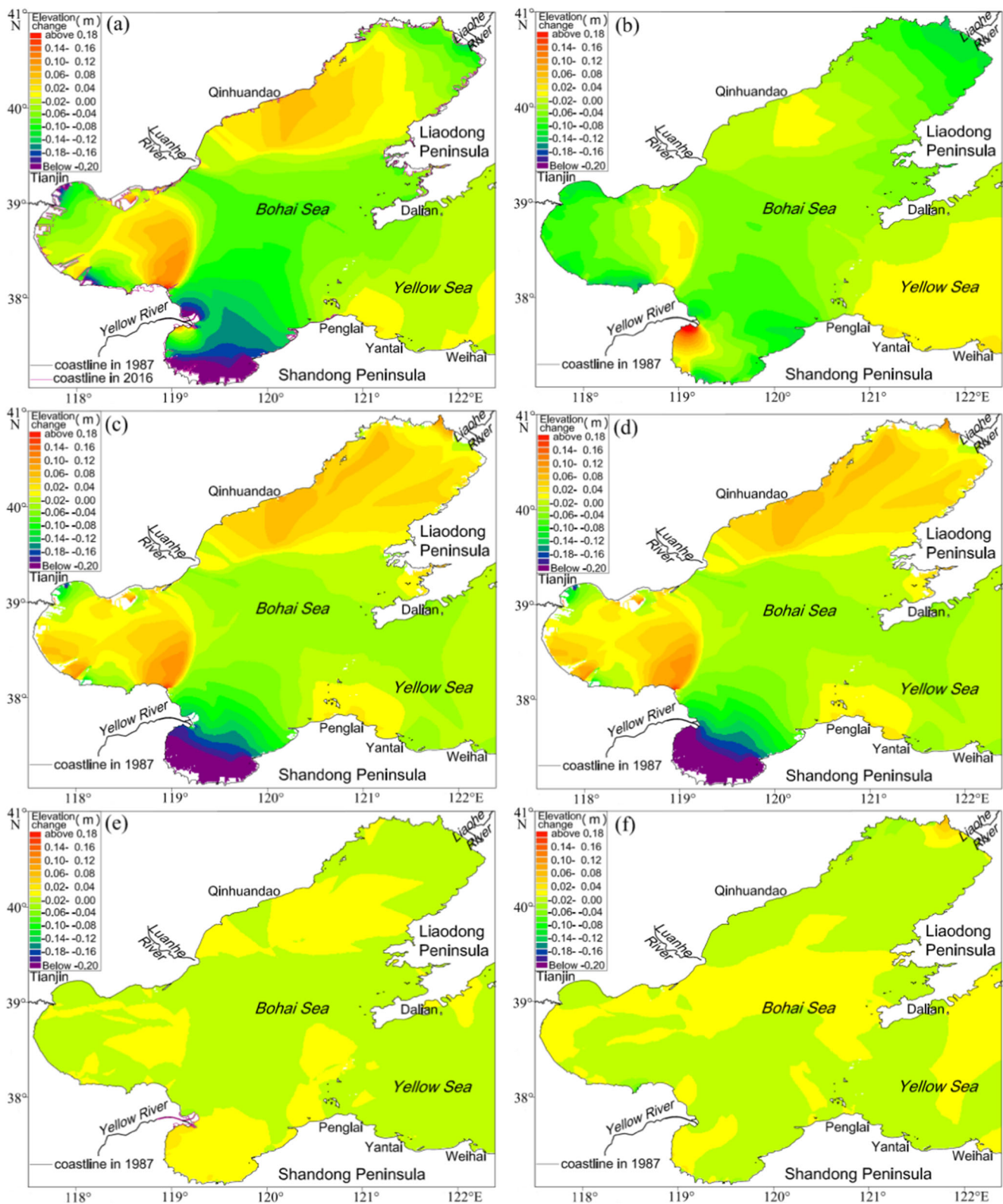


Fig. 11 Variation in the HTL. **a** HTL change from 1987 to 2016. **b** HTL change due to water depth changes. **c** HTL change due to coastline changes. **d** HTL change due to reclamation changes. **e** HTL change due to changes in the Yellow River mouth. **f** HTL changes due to coastal erosion

Changes in the Yellow River and coastal erosion have little effect on the change of the HTL (Fig. 12).

The comparison of the changes in the HTL with the amplitudes of M2, S2, K1, and O1 tidal amplitude and hysteresis

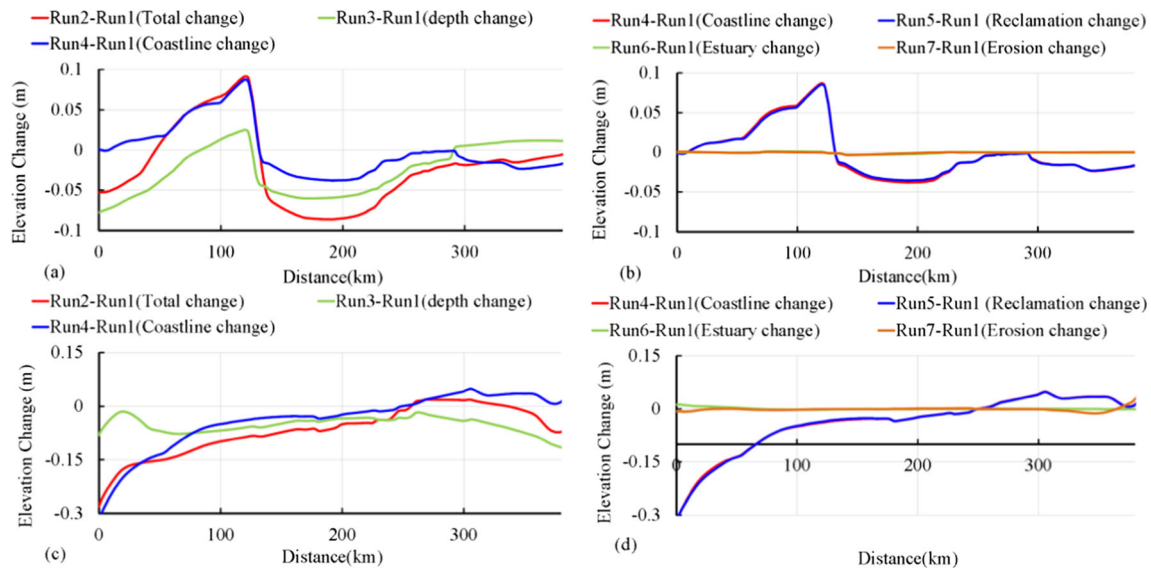


Fig. 12 Comparison of the changes in the HTL in a typical section (see Fig. 4 for the location of the section). **a** Comparison of the changes in the maximum tide levels in the P1-P1' cross-section caused by changes in depth and coastline. **b** Comparison of the changes in the maximum tide levels in the P1-P1' cross-section resulting from changes in reclamation,

the Yellow River estuary, and coastal erosion. **c** Comparison of the changes in the maximum tide levels in the P2-P2' cross-section caused by changes in depth and coastline changes. **d** comparison of the changes in the maximum tide levels in the P2-P2' cross-section resulting from changes in reclamation, the Yellow River estuary, and coastal erosion

shows that the tide level is mainly related to the amplitude change (as shown in Fig. 13a1). Additionally, the correlation with the phase change is small (as shown in Fig. 13a2). The change in the HTL is dominantly due to the change in the tide amplitude of M2, followed by S2, and the influences of the K1 and O1 tides on the change in the HTL are small (Fig. 13a1–d1).

4.2 Tidal flow

The maximum flow velocity has an important influence on the transport of sediment and the erosion and siltation of the seabed. The numerical simulation is divided into 11 layers in the vertical direction. According to the simulation result, the flow velocity of 11 layers of each mesh node is averaged at each hour, and the vertical average flow velocity at that time is obtained. Then, the vertical average flow velocity of each grid node at each time of 721 h in 1 month is calculated. Finally, the maximum value of the vertical average flow velocity at all times of each grid node is proposed, which is the vertical average maximum flow velocity (V_{VAM}).

The simulation results show that the V_{VAM} in the BHS varies from -0.94 to 0.67 m/s from 1987 to 2016 (as shown in Fig. 14a). The V_{VAM} in the western Laizhou Bay has an overall increasing trend, with a maximum flow velocity increase of up to 0.42 m/s. The flow velocity in eastern Laizhou Bay has a decreasing trend, with a maximum flow velocity decrease of 0.45 m/s. The V_{VAM} in the Bohai and Liaodong Bays have decreasing trends, with maximum flow velocity decreases of 0.62 and 0.86 m/s, respectively.

Water depth and coastline changes have different effects on the V_{VAM} . The change in water depth resulted in changes in the V_{VAM} of the BHS ranging from -0.53 to 0.63 m/s (as shown in Fig. 14b). The V_{VAM} in Laizhou Bay has an overall increase trend and the greatest increase in the V_{VAM} is located to the south of the Yellow River mouth, reaching 0.63 m/s. The V_{VAM} in the Bohai and Liaodong Bays have decreasing trends, with decreases of 0.53 and 0.05 m/s, respectively. The V_{VAM} in the Bohai Strait has an overall increasing trend, with the maximum increase of 0.31 m/s occurring the southern part of the Bohai Strait. Due to changes in the coastline, the V_{VAM} of the BHS exhibited changes ranging from -0.88 to 0.62 m/s (Fig. 14c). The V_{VAM} in Laizhou Bay has a decreasing trend, with a maximum decrease of -0.69 m/s. The V_{VAM} in the Bohai Bay has a decreasing trend, with a maximum decrease of 0.65 m/s. The V_{VAM} in Liaodong Bay has an overall increasing trend, with a maximum flow velocity increase of 0.46 m/s. The V_{VAM} in the Bohai Strait has a slight increasing trend, with a maximum increase of 0.08 m/s.

The V_{VAM} variation in the BHS caused by reclamation is basically consistent with the trend and range of the coastline-related velocity change. The V_{VAM} variation is between -0.88 and 0.64 m/s (as shown in Fig. 14d). Changes in the Yellow River mouth and coastal erosion caused relatively small changes in flow velocity, which are mainly limited to the Yellow River estuary or the coastal waters around the coast (Fig. 14e, f).

In order to show the change of flow velocity in the vertical layers, we extracted the maximum of flow velocity of each

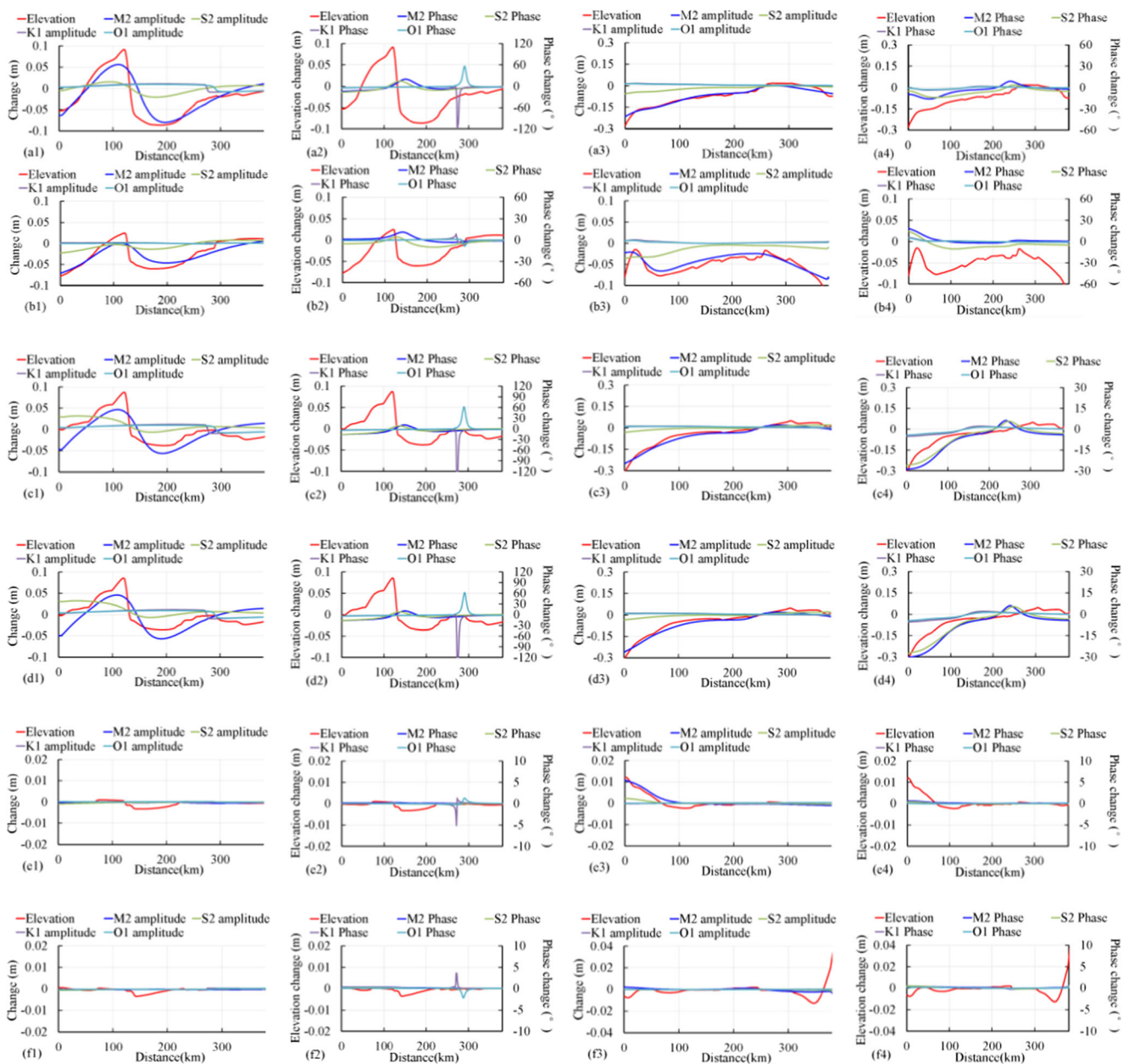


Fig. 13 Curves of the correlation between the HTL variation and the tidal amplitude and phase variation in a typical section (see Fig. 4 for the location of the section). **a1–a4** Comparison of the overall changes from 1987 to 2016; **a1, a2** P1-P1' section, **a3, a4** P2-P2' section. **b1–b4** Comparison of water depth changes; **b1, b2** P1-P1' section, **b3, b4** P2-P2' section. **c1–c4** Comparison of coastline changes; **c1, c2** P1-P1'

section, **c3, c4** P2-P2' section. **d1–d4** Comparison of reclamation effects; **d1, d2** P1-P1' section, **d3, d4** P2-P2' section. **e1–e4** Comparison of effects of changes in the Yellow River estuary; **e1, e2** P1-P1' section, **e3, e4** P2-P2' section. **f1–f4** Comparison of coastline erosion effects; **f1, f2** P1-P1' section; **f3, f4** P2-P2' section

mesh node in the surface, middle, and bottom layers in 1 month (721 h), called the maximum flow velocity (V_{\max}). The absolute change of V_{\max} is the V_{\max} in 2016 minus the V_{\max} in 1987 ($V_{\max-2016} - V_{\max-1987}$). The relative changes of V_{\max} is $(V_{\max-2016} - V_{\max-1987})/V_{\max-2016} \times 100$. Then, the area corresponding to the relative change value and the absolute change value of V_{\max} is counted, respectively. The ratio of the area to the total area of the Bohai Sea is the relative change rate in area.

According to Fig. 15, the curves of the absolute and relative changes in the maximum flow velocity in the surface, middle, and bottom layers to the area of the BHS (at 1 cm/s and 1% intervals, respectively) are roughly normal and logarithmic. The relationship between the absolute value of the maximum flow velocity at each stage and the area of the BHS gradually decreases from the surface to the bottom, and the relative change values are basically the same. For example, areas with decreasing flow velocity values between 4 and 5 cm/s in the

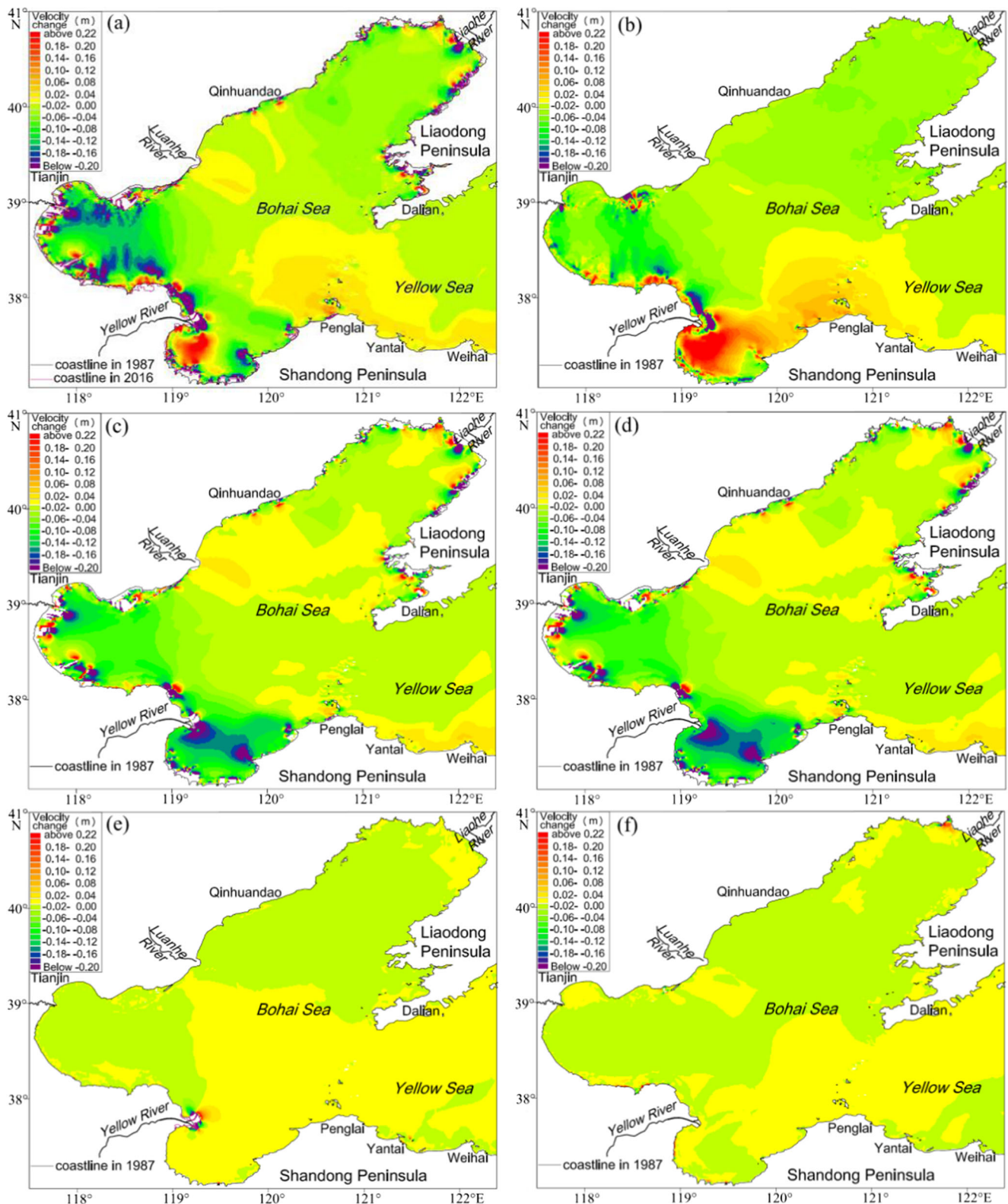


Fig. 14 V_{VAM} changes. **a** V_{VAM} change from 1987 to 2016. **b** V_{VAM} change due to water depth change. **c** V_{VAM} change due to coastline change. **d** V_{VAM} change due to reclamation. **e** V_{VAM} change due to changes in the Yellow River. **f** V_{VAM} change due to coastal erosion

surface, middle, and bottom layers account for 5.5, 5.2, and 3.4% of the BHS area, respectively. Additionally, areas with relative changes between 4 and 5% in the surface, middle, and

bottom layers account for 4.5, 4.4, and 4.4% of the BHS, respectively (as shown in Fig. 15a). The change in water depth resulted in the largest change in the absolute value of middle

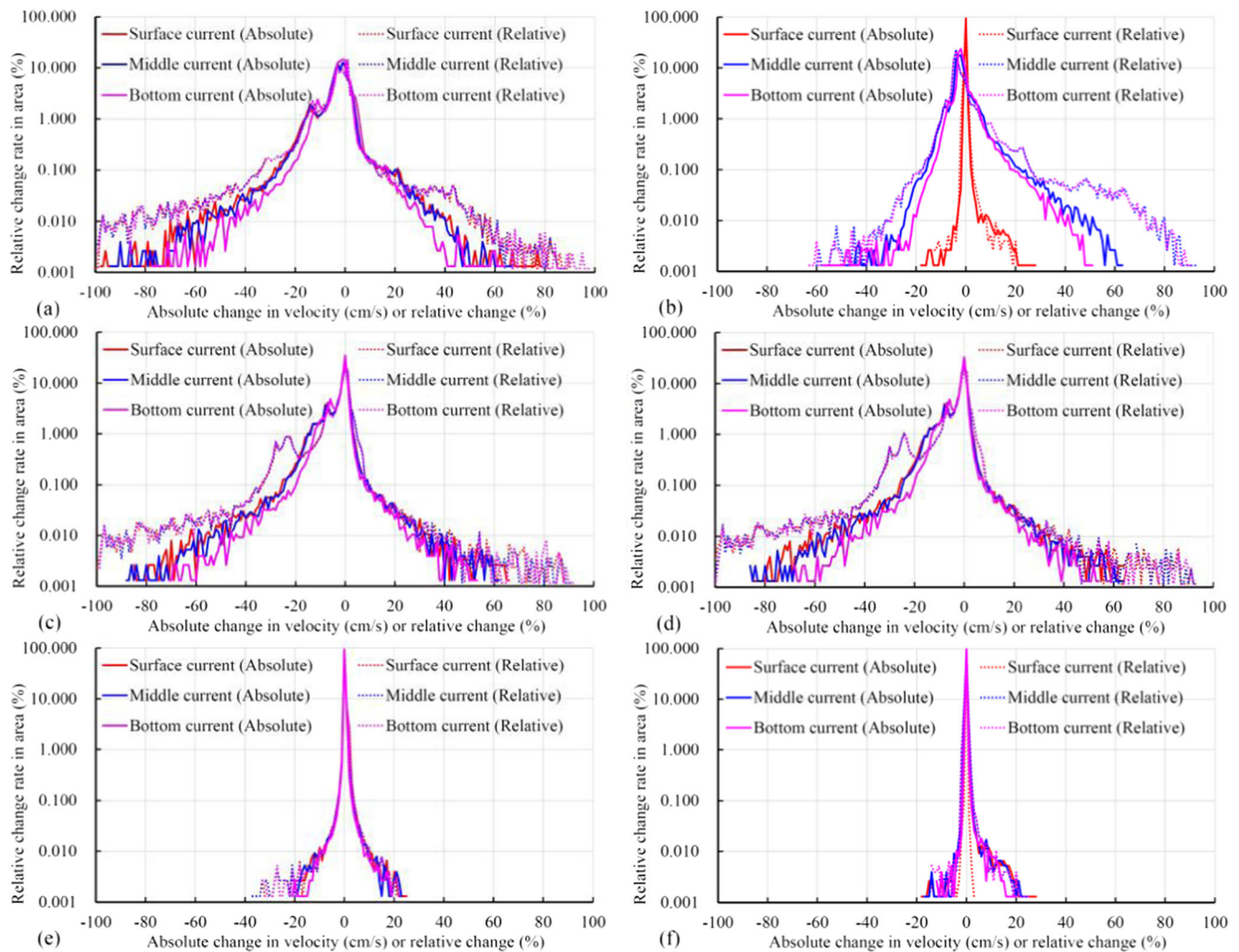


Fig. 15 V_{\max} changes in the surface, middle, and bottom layers versus corresponding area curves. **a** V_{\max} change from 1987 to 2016. **b** V_{\max} change due to water depth change. **c** V_{\max} change due to coastline change.

d V_{\max} change due to reclamation. **e** V_{\max} change due to changes in the Yellow River. **f** V_{\max} change due to coastal erosion

layer velocity, followed by the bottom layer velocity, whereas the change in the surface flow velocity was small. The relative changes in the bottom and middle velocities were basically the same, but the relative change in the surface velocity was obviously smaller (as shown in Fig. 15b). Changes in the coastline caused the absolute values of the surface and middle layers to be greater than that of the bottom layer, and the relative changes in the three layers were basically the same. The trend and area of the flow velocity caused by reclamation are basically the same as those of the changes in the coastline. The absolute and relative changes in the surface, middle, and bottom flows caused by the changes in the Yellow River mouth and coastal erosion are not significantly different.

The comparison of the V_{\max} in the P1-P1' and P2-P2' cross-sections reveals that when the flow velocity changes caused by water depth changes and coastline changes decrease or increase together, the flow velocity change is magnified (see Fig. 16a). However, when the flow velocity changes caused

by the changes in the water depth and coastline are opposite, the flow velocity changes exhibit a cancelation effect (see Fig. 16c). The change trend of the flow velocity caused by reclamation is basically the same as that of the coastline change, and changes in the Yellow River estuary and coastal erosion are responsible for only a small change in flow velocity (as shown in Fig. 16b, d).

4.3 Residual currents

In this paper, the Euler residual flow principle is used to calculate the residual flow based on the numerical results for 1 month (Fig. 17). The residual currents display an overall increasing trend from 1987 to 2016 in the BHS. Due to the changes in the Yellow River estuary and the construction of nearshore projects, the residual flow velocities in the waters near the Yellow River estuary and the nearshore projects have increased considerably, with a maximum increase of 0.32 m/s.

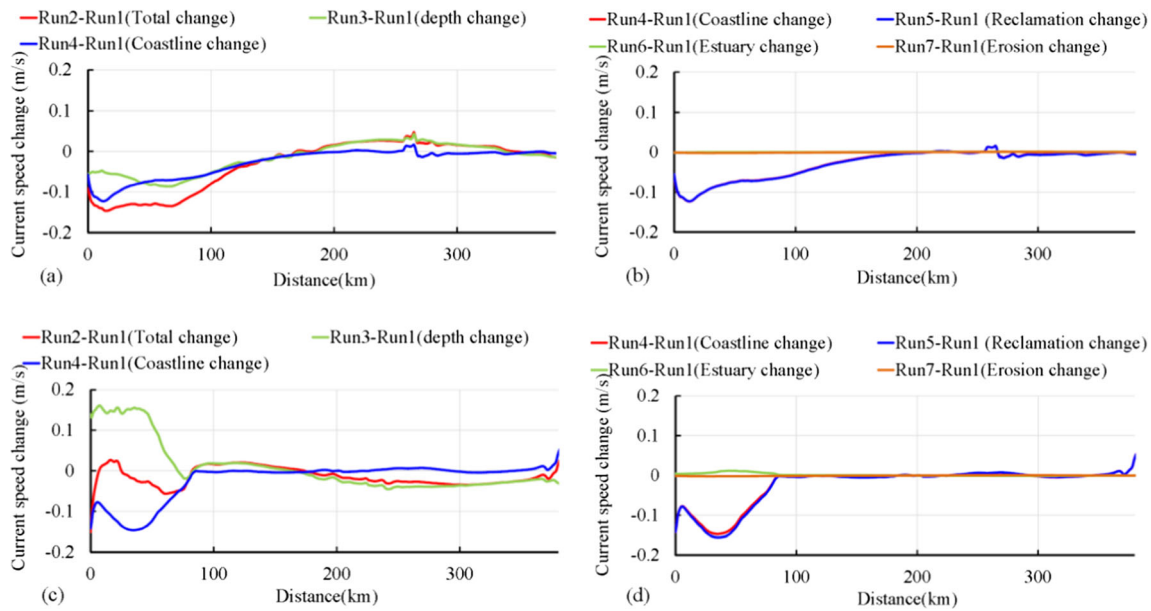


Fig. 16 Comparison of the V_{max} changes in a typical section (see Fig. 4 for cross-section positions). **a** Comparison of the V_{max} changes in the P1-P1' cross-section due to changes in depth and coastline. **b** Comparison of the V_{max} changes in the P1-P1' cross-section due to changes in reclamation, the Yellow River, and coastal erosion. **c** Comparison of the

V_{max} changes in the P2-P2' cross-section due to changes in depth and coastline. **d** Comparison of the V_{max} changes in the P2-P2' cross-section due to changes in sea reclamation, the Yellow River mouth, and coastal erosion

The increases in the residual flow velocities in the middle of the Laizhou, Liaodong, and Bohai Bays are generally between 0.01 and 0.05 m/s.

Through the analysis of the relationship between the residual current changes and the proportion of occupied BHS area, we can see that the residual current changes have a normal distribution and show a logarithmic change relationship (see Fig. 18). Among the influencing factors of coastal transition, reclamation is the main factor leading to changes in the velocity of the residual current in the BHS, followed by changes in the Yellow River and coastal erosion.

4.4 Tidal fluxes

The tidal flux refers to the amount of seawater that passes through a section during the flood tide and ebb tide. Tidal flux

is one of the important indicators reflecting the transport flux of sediment and pollutants in the Gulf. It is often used to study the impact of engineering construction on seawater exchange in the Gulf (Jiang et al. 2015; Li et al. 2014a, b). To study the overall effects of the changes in the coastline of the BHS, four profile (P-LZB, P-BHB, P-P-LDB, and P-BHS) were selected to calculate the tidal flux of the BHS during the spring tide period. Table 5 shows that the changes in the coastline from 1987 to 2016 influenced the changes in flux in the bay of BHS. The maximum change in the tidal flux appears in the P-LZB profile, where the flood and ebb tidal fluxes are reduced by $58.57 \times 10^8 \text{ m}^3/\text{day}$ (20.53%) and $62.88 \times 10^8 \text{ m}^3/\text{day}$ (22.09%), respectively. The minimum change in the tidal flux appears in the P-LDB profile, where the flood and ebb tidal fluxes decreased by $4.85 \times 10^8 \text{ m}^3/\text{day}$ (0.63%) and $9.37 \times 10^8 \text{ m}^3/\text{day}$ (1.21%), respectively.

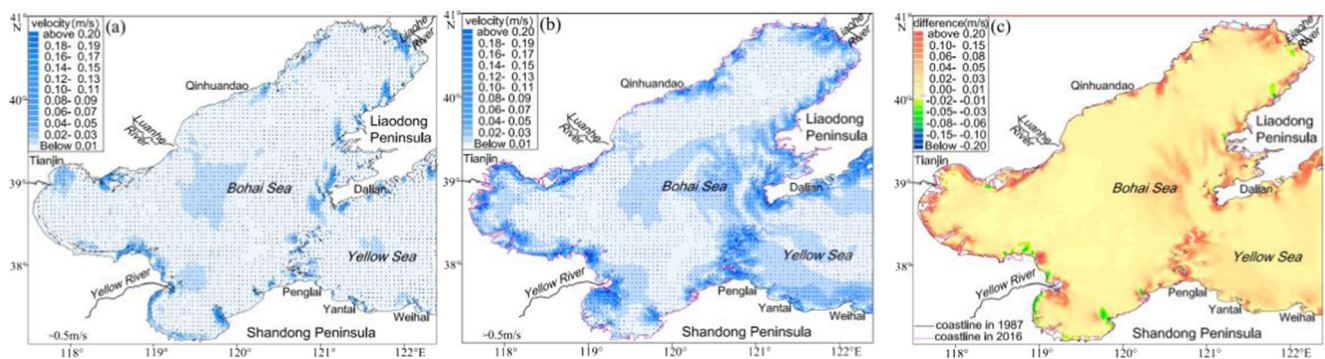


Fig. 17 Changes in the residual currents between 1987 and 2016. **a** Residual current velocity in 1987. **b** Residual current velocity in 2016. **c** Differences in the residual currents (2016–1987)

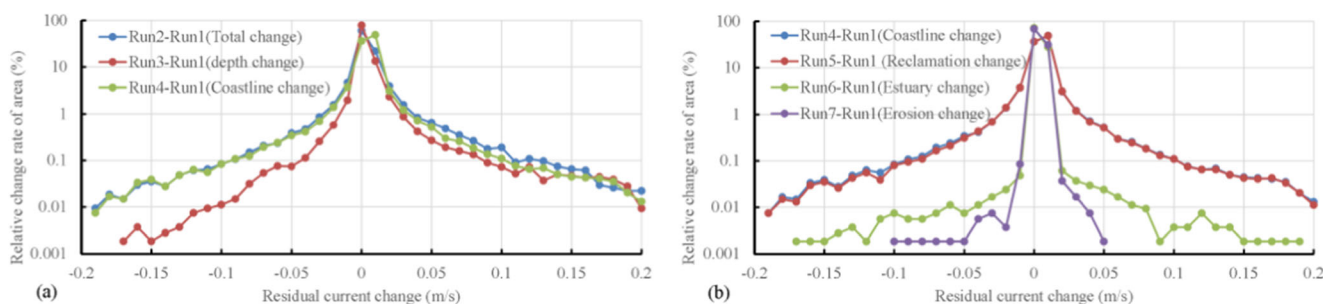


Fig. 18 The relationship between the relative change in residual flow velocity and the proportion of occupied Bohai Sea area. **a** Changes in the residual flow velocities due to changes in water depth and coastline. **b**

Changes in the residual flow velocities caused by reclamation, changes in the Yellow River, and coastal erosion

From 1987 to 2016, the coastline change played a major role in the overall change in the tidal flux in Laizhou Bay. The impact of coastline and water depth changes on the tidal flux was basically the same as the overall changes in the tidal flux in Bohai Bay. The effect of the water depth change dominates the overall change in the tidal flux in Liaodong Bay (as shown in Fig. 19a). Among the coastal changes, reclamation is the factor controlling the changes in the tidal flux and coastline changes and coastal erosion have little impact on the tidal flux (Fig. 19b).

5 Discussion

In this paper, the variation of tidal dynamics in the Bohai Sea from 1987 to 2016 was studied by numerical simulation. Quantitative study of tidal dynamics under the influence of different factors such as water depth change, coastline change, reclamation, coastal erosion and Yellow River estuary changes. The results show that the Bohai Sea half-day tidal wave system has undergone major changes in the past 30 years, and the daily tidal wave system has changed little (as shown in Table 6).

The half-day tidal amplitude generally showed an increasing trend (as in Table 6, ①). The areas where the M_2 and S_2 tidal amplitudes increased by 10% accounted for 32.85–35.66% of the Bohai Sea area, and the area where the amplitude decreased by more than 10% accounted for 4.71–5.47%

of the Bohai area. The amplitude of the full-day tidal wave is slightly reduced (as in Table 6, ①), the area where the tidal amplitude is reduced accounts for 3.28–3.60% of the Bohai Sea area, and the area where the amplitude increases by 10% accounts for 1.16–1.33% of the Bohai Sea area. The average depth of the BHS is calculated to be approximately 18 m, the wavelength of the half-wave of M_2 is approximately 590 km, and the wavelength of the tide of K_1 is approximately 1140 km. If the BHS is regarded as a semi-enclosed bay, the bay mouth is the Bohai Strait, and the distance from the bay mouth to the head of Bohai Bay is approximately 270 km, which is approximately 1/2 and 1/4 of the half-wave tides of M_2 and K_1 , respectively. After the reclamation in Bohai Bay, the change in the coastline at the head of Bohai Bay has a greater influence on the half-day than of the full-day tidal wave. Therefore, although the influence of the coastline changes within the BHS on the half-day tidal wave is relatively large, these changes have little effect on the full-day tidal wave.

The effects of water depth changes and coastline changes on the tidal wave system of the Bohai Sea have mutually offset effects, and the effects of mutual coupling are less than the linear superposition of individual factors (see in Table 6, ⑤). The change of water depth mainly affects the half-day tide of the Bohai Sea. The contribution of water depth change to the increase of M_2 and S_2 tidal amplitude is 48.18–72.24% (as shown in Table 6, ⑥). The contribution rate of coastline changes to the increase of the half-day tidal amplitude of the

Table 5 The tidal flux of the BHS during the flood and ebb periods of the spring tide in 1987 and 2016 ($\times 10^8 \text{ m}^3/\text{day}$)

| Profile | | Run1 (1987) | Run2 (2016) | Run3 (depth) | Run4 (coastline) | Run5 (reclamation) | Run6 (estuary) | Run7 (erosion) |
|---------|--------------------|-------------|-------------|--------------|------------------|--------------------|----------------|----------------|
| P-LZB | Flood tide(inward) | 285.21 | 226.64 | 261.95 | 228.14 | 227.15 | 285.98 | 285.79 |
| | Ebb tide(outward) | 284.69 | 221.81 | 259.28 | 229.20 | 227.56 | 285.27 | 284.89 |
| P-BHB | Flood tide(inward) | 516.36 | 484.69 | 495.73 | 493.41 | 493.21 | 515.96 | 516.07 |
| | Ebb tide(outward) | 509.34 | 476.82 | 488.67 | 484.97 | 484.76 | 509.00 | 509.17 |
| P-LDB | Flood tide(inward) | 768.22 | 763.37 | 739.92 | 775.35 | 775.05 | 768.87 | 766.89 |
| | Ebb tide(outward) | 774.69 | 765.32 | 743.68 | 783.21 | 782.59 | 774.00 | 773.33 |

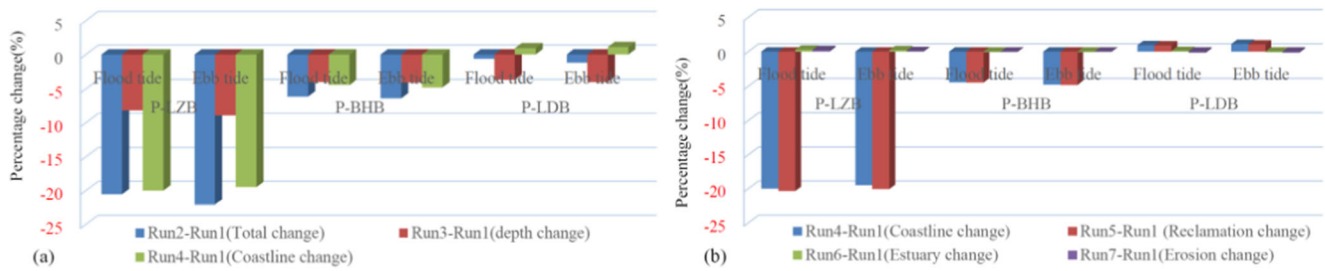


Fig. 19 Percentage changes in the tidal flux. **a** Percentage changes in the tidal flux due to changes in water depth and coastline. **b** Percentage changes in the tidal flux due to reclamation, changes in the Yellow River, and coastal erosion

Bohai Sea is 27.76–51.82%, the contribution rate to the half-day tidal amplitude reduction is 83.68–96.35%, and the contribution rate to the full-day tidal amplitude variation is 96.35–99.07% (as shown in Table 6, ⑦).

Channel excavation, sand mining, and submarine erosion increase the water depth, whereas the deposition of sediments from the Yellow River decreases the water depth. The deposition of sediment from the Yellow River led to a maximum shallowing of 12.4 m in the southern waters, an increase of 0.25 m in the maximum tide level, and a maximum increase of 0.63 m/s in the flow velocity. The water depth deepened by 5.6 m in the southern part of Bohai Bay, the value of the HTL decreased by 0.16 m, and the maximum flow velocity decreased by 0.27 m/s. Therefore, shallower water depth led to increased bottom friction, a higher maximum tide level, and a higher maximum flow velocity. Deeper water depth resulted in less bottom friction, a lower maximum tide level, and a lower maximum flow velocity.

In the past 30 years, the change of coastline has led to an increase of 0.19 m of HTL and an increase of 0.62 m/s of V_{VAM} in the Bohai Sea. An increase in the HTL increases the risk of coastal erosion and marine disasters (Ding and

Wei 2017). The increase in V_{VAM} will change the transport flux of sediment (Gao et al. 2017), which has an impact on the erosion and erosion patterns of the Bohai Sea. The change of the coastline leads to the maximum increase of the residual flow velocity of 0.32 m/s. The change of the residual flow will change the transport law of pollutants and sediment, and thus affect the transport flux of sediment and pollutants. The change of coastline caused the tidal flux in Laizhou Bay to decrease by 19.49–22.01%. The reduction of water exchange rate will increase the exchange time of water bodies in the bay, which is not conducive to the purification of water quality, leading to deterioration of the ecological environment (Li et al. 2013). Factors affecting coastline changes include reclamation, coastal erosion, and the Yellow River Estuary changes. The reclamation is the dominant factor leading to the change of coastline, and its contribution rate to coastline changes reaches 99.55–99.91% (as shown in Table 7, ⑦). The tidal waves in narrow and long semi-enclosed bays are formed by the superposition of incident waves from the outer sea and reflection waves from reflections at the bay’s head. The water depth of the original seabed is relatively flat. When the incident tidal wave propagates to the shore, energy is gradually

Table 6 Amplitude change accounts for the proportion of the Bohai Sea area (%) and the influence level of the water depth and shoreline changes (%) from 1987 to 2016

| Constituent | Amplitude change | ① | ② | ③ | ④ | ⑤ | ⑥ | ⑦ |
|-------------|------------------|--------------------------|--------------------------|------------------------------|-------|--------|-----------|-----------|
| | | Run2-Run1 (total change) | Run3-Run1 (depth change) | Run4-Run1 (coastline change) | ② + ③ | ① - ④ | ②/④ × 100 | ③/④ × 100 |
| M2 | Increase (> 10%) | 35.66 | 24.83 | 26.71 | 51.54 | -15.88 | 48.18 | 51.82 |
| | Decrease (> 10%) | 5.47 | 1.16 | 5.97 | 7.14 | -1.67 | 16.32 | 83.68 |
| S2 | Increase (> 10%) | 32.85 | 26.06 | 10.02 | 36.08 | -3.23 | 72.24 | 27.76 |
| | Decrease (> 10%) | 4.71 | 0.68 | 17.85 | 18.53 | -13.82 | 3.65 | 96.35 |
| K1 | Increase (> 10%) | 1.16 | 0.04 | 1.51 | 1.56 | -0.39 | 2.80 | 97.20 |
| | Decrease (> 10%) | 3.60 | 0.03 | 3.68 | 3.71 | -0.11 | 0.93 | 99.07 |
| O1 | Increase (> 10%) | 1.33 | 0.03 | 1.71 | 1.74 | -0.41 | 1.99 | 98.01 |
| | Decrease (> 10%) | 3.28 | 0.04 | 3.11 | 3.15 | 0.14 | 1.20 | 98.80 |

consumed. It is not easy to form total reflections at the head of the bay to generate standing waves. After the construction of a reclamation project, the coastline is mostly upright and the slope is relatively steep. Steep breakwaters have low energy consumption and are more susceptible to total reflection of incident tidal waves, forming standing waves (Pelling et al. 2013). Reclamation will accelerate the propagation of tidal waves to some extent. The contribution rate of coastal erosion to coastline changes is only 0.05–0.40% (see Table 7, ⑨). The contribution rate of estuary changes to coastline changes is only 0.01–0.12% (as shown in Table 7, ⑧). Therefore, strictly controlling the scale of reclamation are important measures for reducing the decline in water exchange capacity and the deterioration of the ecological environment.

We collected the bathymetric data of sea charts published in 1984–1994 and 2007–2014. Because the Bohai Sea area is 77,000 km² (Ding and Wei 2017), it is difficult to obtain water depth data for 1 year in the Bohai Sea. There are large differences in water depth measurements in different regions. For example, the water depths in the central part of the Bohai Sea and the central part of the Liaodong Bay are mainly from the 1950s to the 1990s. Water depth data around 2016 is not collected. There is no objective reflection of the water depth changes in Liaodong Bay in the past 30 years. Therefore, the simulation results show that the tidal changes in Liaodong Bay are small.

The tidal level verification was carried out in the simulation results of 1987 and 2016, respectively. In this paper, the measured tide level data of various tide stations were not collected, and the harmonic constant data was mainly collected. The duration of the tide level observation was generally 1 month. In addition, the observation time of tidal level data is quite different. The tidal observation time used for tidal level verification in 1987 was from 1975 to 1990, and the tidal observation time for tidal level verification in 2016 was from 2007 to 2016. At the same time, there are differences in the positions of tidal stations at different times. Therefore, some station simulations and measured harmonic constants have large errors. In order to facilitate comparative analysis, the open boundary of the simulation adopted a unified tidal level, and the influence of the depth of the Yellow Sea and the variation of the shoreline on the open boundary was not considered, and the simulation result was also affected. At the same time, this paper does not consider the effects of sea level rise, wind and waves, changes in runoff and sediment volume of the Yellow River, and does not fully reflect the tidal dynamic changes of the Bohai Sea. For example, according to a simulation of the western Pacific tidal waves performed using a mathematical model, the maximum increase in the tidal range along the coast of China is expected to be approximately 0.4 m after the sea level rises by 0.90 m (Zhang et al. 2013). The change in sea level has been 4.93 mm/year over nearly 10 years in the East China Sea. According to this estimate, the rise in sea level

Table 7 Amplitude change, which is caused by coastline changes, accounts for the proportion of the Bohai Sea area (%) and influence level of different factors (%) from 1987 to 2016

| Constituent | Amplitude change | ① | ② | ③ | ④ | ⑤ | ⑥ | ⑦ | ⑧ | ⑨ |
|-------------|--------------------------------------|---------------------------------|-----------------------------------|-------------------------------|-------------------------------|-----------|-------|-----------|-----------|-----------|
| | | Run4-Run1 (coastline change) | Run5-Run1 (reclamation change) | Run6-Run1 (estuary change) | Run7-Run1 (erosion change) | ② + ③ + ④ | ① - ⑤ | ②/⑤ × 100 | ③/⑤ × 100 | ④/⑤ × 100 |
| M2 | Increase (> 10%) Decrease (> 10%) | 26.71 | 26.74 | 0.003 | 0.021 | 26.76 | -0.05 | 99.91 | 0.01 | 0.08 |
| S2 | Increase (> 10%) Decrease (> 10%) | 5.97 | 5.92 | 0.003 | 0.024 | 5.94 | 0.03 | 99.55 | 0.05 | 0.40 |
| K1 | Increase (> 10%) Decrease (> 10%) | 10.02 | 10.35 | 0.004 | 0.012 | 10.37 | -0.35 | 99.85 | 0.04 | 0.11 |
| O1 | Increase (> 10%) Decrease (> 10%) | 17.85 | 18.63 | 0.002 | 0.015 | 18.64 | -0.79 | 99.91 | 0.01 | 0.08 |
| | Increase (> 10%) Decrease (> 10%) | 1.51 | 1.47 | 0.001 | 0.003 | 1.48 | 0.04 | 99.73 | 0.07 | 0.20 |
| | Increase (> 10%) Decrease (> 10%) | 3.68 | 3.69 | 0.001 | 0.002 | 3.69 | -0.01 | 99.92 | 0.03 | 0.05 |
| | Increase (> 10%) Decrease (> 10%) | 1.71 | 1.68 | 0.002 | 0.002 | 1.68 | 0.02 | 99.76 | 0.12 | 0.12 |
| | Increase (> 10%) Decrease (> 10%) | 3.11 | 3.07 | 0.003 | 0.004 | 3.07 | 0.04 | 99.77 | 0.10 | 0.13 |

in the BHS over nearly 30 years is approximately 14.8 cm, and the maximum increase in the tidal range near the shore is approximately 6.6 cm. In the future research, it is necessary to collect data such as water depth, tidal level, and tidal current in the same year, and consider coupling simulations such as sea level rise, tidal current, wave and sediment transport, and comprehensively and accurately reveal the impact of coastline changes on tidal dynamics and sediment transport.

In this paper, three-dimensional tidal current models with the refined grid is used to quantitatively study the tidal dynamics under the influence of different factors such as water depth change, coastline change, reclamation, coastal erosion, and Yellow River Estuary change. The study is of great significance for further improving the research results of the interaction mechanisms between human activities and tidal dynamics.

6 Conclusions

Over the past 30 years, due to the construction of ports and changes in the mouth of the Yellow River, the BHS coastline has undergone considerable changes. In this paper, Landsat satellite remote sensing images are used to extract the coastlines of the BHS in 1987 and 2016. A three-dimensional tidal current model of the BHS and the Yellow Sea is constructed using the MIKE 3 model. The results show that the model results are reliable and can be used to study the influence of coastline variations on the tidal current fields in the BHS.

We simulated and analyzed the effects of changes in coastline, depth, topography, reclamation projects, the Yellow River estuary, and coastal erosion on tidal systems, tide levels, tidal currents, residual currents, and tidal fluxes. The results show that the half-day tides of the BHS have changed considerably and that the variation in the M2 tidal amplitude is between -0.233 and 0.172 m. The change in the daily tide is small, and the change in the K1 tidal amplitude is between -0.009 and 0.031 m. The two M2 amphidromic points and the one K1 amphidromic point in the BHS have migrated by between 4.6 and 16 km. The relative changes in the amplitudes of the half-day tides (M2 and S2) are basically the same. The relative changes in the amplitudes of the full-day tides (K1 and O1) are also basically the same. However, the relative changes in tidal amplitude are greater for the half-day than for the whole-day tide. The changes in tidal amplitudes of M2, S2, K1, and O1 caused by coastline changes accounted for 27.76–99.07% of the overall change in amplitude from 1987 to 2016, and water depth changes accounted for 0.93–72.24% of the overall change. The HTL in the BHS changed by between -0.32 and 0.21 m. The V_{VAM} in the BHS changed by -0.94 to 0.67 m/s from 1987 to 2016. The maximum change in the residual current is 0.32 m/s. The maximum change in the tidal flux occurred in Laizhou Bay (P-LZB), and the minimum

change in the tidal flux occurred in Liaodong Bay (P-LDB), where the tidal fluxes decreased by 20.53–22.09 and 0.63–1.21%, respectively.

In conclusion, the tidal wave system, tide levels, tidal currents, residual flows, and tidal fluxes of the BHS have changed somewhat. The largest changes have occurred in Laizhou Bay, followed by the Bohai and Liaodong Bays. The amount of change in the tidal dynamics is proportional to the degree of change in the coastline. The changes in the tidal flux are related to the changes in the area of the bay, the changes in the coastline at the bay mouth, and the tortuosity of the original coastline. The dominant factor driving coastline changes is reclamation, accounting for 99.55–99.91% of the amplitude changes in tidal waves, followed by coastal erosion, accounting for 0.05–0.40% of tidal wave amplitude changes. The contribution of changes in the Yellow River mouth to the tidal wave amplitude changes is small, accounting for 0.01–0.12% of the amplitude changes. The change in the HTL is mainly related to the amplitude change, and the correlation with the phase change is small. The dominant factor responsible for the change in the HTL is the change in the tide amplitude of M_2 , followed by S_2 , whereas the influence of the K_1 and O_1 tides on the change in the HTL is small. The absolute value of the maximum flow velocity gradually decreases from the surface to the bottom, and the relative change value is basically the same. As the tidal flux decreases, the water exchange capacity of the BHS decreases, which has an impact on the ecological environment of the BHS. Therefore, strictly controlling the scale of reclamation are important measures for reducing the decline in water exchange capacity and the deterioration of the ecological environment.

Acknowledgments This work was supported by the National Natural Science Foundation of China (grant number 41776059). We thank Professor Jiang Wensheng of Ocean University of China for providing many valuable opinions and suggestions for this paper. We also thank the expert reviewers for their valuable suggestions.

References

- Chu Z, Sun XG, Zhai SK, Xu KH (2006) Changing pattern of accretion/erosion of the modern Yellow River (Huanghe) subaerial delta, China: based on remote sensing images. *Mar Geol* 227:13–30
- Danish Hydraulic Institute (2016) MIKE 3 flow model FM hydrodynamic module user guide. Danish
- Ding Y, Wei H (2017) Modeling the impact of land reclamation on storm surges in Bohai Sea, China. *Nat Hazards* 85(1):559–573
- Editorial Board Marine Atlas (1994) Marine atlas of Bohai Sea, Yellow Sea and East China Sea. China Ocean Press, Beijing
- Flemming BW, Nyandwi N (1994) Land reclamation as a cause of fine-grained sediment depletion in backbarrier tidal flats (southern North Sea). *Neth J Aquat Ecol* 28(3–4):299–307
- Gao GD, Wang XH, Bao XW (2014) Land reclamation and its impact on tidal dynamics in Jiaozhou Bay, Qingdao, China. *Estuar Coast Shelf Sci* 151:285–294

- Gao GD, Wang XH, Bao XW, Song D, Lin XP, Qiao LL (2017) The impacts of land reclamation on suspended-sediment dynamics in Jiaozhou Bay, Qingdao, China. *Estuar Coast Shelf Sci* 206:1–15
- Gu D, Zhang Y, Fu J, Zhang X (2007) The landscape pattern characteristics of coastal wetlands in Jiaozhou Bay under the impact of human activities. *Environ Monit Assess* 124(1–3):361–370
- Hu H, Yuan Y, Wan Z (2004) Study on hydrodynamic environment of the Bohai Sea, the Huanghai Sea and the East China Sea with wave-current coupled numerical model. *Acta Oceanol Sin* 26(4):19–32
- Huang Z (1991) Tidal waves in the Bohai Sea and their variations. *J Ocean Univ China* 21(2):1–12
- Jabaloy-Sánchez A, Lobo FJ, Azor A (2010) Human-driven coastline changes in the Adra River deltaic system, Southeast Spain. *Geomorphology* 119:9–22
- Jiang W (2004) SPM transport in the Bohai Sea field experiments and numerical modelling. *J Mar Syst* 44:175–188
- Jiang W, Pohlmann T, Sundermann JR (2000) A modelling study of SPM transport in the Bohai Sea. *J Mar Syst* 24:175–200
- Jiang SH, Zhu LH, Hu RJ, Zhang W, Liu AJ (2015) The hydrodynamic response to reclamation in Laizhou Bay. *Period Ocean Univ China* 45(10):074–080
- Li S, Wang N, Zhang Y, Nan-qí S (2013) Ecological impacts of marine reclamation in Bohai Sea from 1981 to 2011. *Mar Environ Sci* 32(6):926–929
- Li L, Wang XH, Andutta F, Williams D (2014a) Effects of mangroves and tidal flats on suspended-sediment dynamics: observational and numerical study of Darwin harbour, Australia. *J Geophys Res Oceans* 119:5854–5873
- Li P, Li G, Qiao L, Chen X, Shi J, Gao F, Wang N, Yue S (2014b) Modeling the tidal dynamic changes induced by the bridge in Jiaozhou Bay, Qingdao, China. *Cont Shelf Res* 84:43–53
- Liu Z, Wei H, Jiang S (2003) Characteristics of seasonal variation of monthly mean temperature and salinity fields in the Bohai Sea and analysis of the related dynamics. *J Ocean Univ China* 33(1):007–014
- van Maren DS, Oost AP, Wang ZB, Vos PC (2016) The effect of land reclamations and sediment extraction on the suspended sediment concentration in the ems estuary. *Mar Geol* 376:147–157
- Nichols FH, Cloern JE, Luoma SN, Peterson DH (1986) The modification of an estuary. *Science* 231(4738):567–573
- Pardo-Pascual JE, Almonacid-Caballer J, Ruiz LA (2012) Automatic extraction of shorelines from Landsat TM and ETM+ multi-temporal images with subpixel precision. *Remote Sens Environ* 123:1–11
- Parker DS, Norris DP, Nelson AW (1972) Tidal exchange at Golden Gate. *J Sanit Eng Div* 98(2):305–323
- Pelling HE, Uehara K, Green JAM (2013) The impact of rapid coastline changes and sea level rise on the tides in the Bohai Sea, China. *J Geophys Res Oceans* 118(7):3462–3472
- Qian C, Sheng Y (2000) Distribution of 9 principal tidal constituents and tide prediction for the East China Sea. *China Ocean Eng* 14(04):541–548
- Ren ME, Shi YL (1986) Sediment discharge of the Yellow River (China) and its effect on the sedimentation of the Bohai and the Yellow Sea. *Cont Shelf Res* 6(6):785–810
- Shen C, Shi H, Zheng W, Li F, Peng S, Ding D (2016) Study on the cumulative impact of reclamation activities on ecosystem health in coastal waters. *Mar Pollut Bull* 103(1–2):144–150
- Song D, Wang XH (2013) Suspended sediment transport in the Deepwater Navigation Channel, Yangtze River estuary, China, in the dry season 2009: 2. Numerical simulations: SS Transport in Dnc Yre. *J Geophys Res Oceans* 118(10):5568–5590
- Takekawa JY, Woo I, Spautz H (2006) Environmental threats to tidal-marsh vertebrates of the San Francisco Bay estuary. *Stud Avian Biol* 32:176–197
- Tian B, Wu W, Yang Z, Zhou Y (2016) Drivers, trends, and potential impacts of long-term coastal reclamation in China from 1985 to 2010. *Estuar Coast Shelf Sci* 170:83–90
- Wang K, Fang G, Feng S (1999) A 3-D numerical simulation of M2 tides and tidal currents in the Bohai Sea, the Huanghai Sea and the East China Sea. *Acta Oceanol Sin* 21(4):1–13
- Wang H, Yang Z, Saito Y, Liu JP, Sun X (2006) Interannual and seasonal variation of the Huanghe (Yellow River) water discharge over the past 50 years: connections to impacts from ENSO events and dams. *Glob Planet Chang* 50(3–4):212–225
- Wang H, Yang Z, Saito Y, Liu JP, Sun X, Wang Y (2007) Stepwise decreases of the Huanghe (Yellow River) sediment load (1950–2005): impacts of climate change and human activities. *Glob Planet Chang* 57(3–4):331–354
- Wang JN, Meng YH, Zhang LX (2016) Remote sensing monitoring and change analysis of Yellow River estuary coastline in the past 42 years. *Remote Sens Land Resour* 28(3):188–193
- White K, El Asmar HM (1999) Monitoring changing position of coastlines using thematic mapper imagery, an example from the Nile Delta. *Geomorphology* 29(1):93–105
- Xiong X (2012) China's offshore ocean—physical oceanography and marine meteorology. Ocean Press, Beijing
- Yanagi T, Ohnishi K (1999) Change of tide, tidal current, and sediment due to reclamation in Tokyo Bay. *Oceanogr Jpn* 8:411–415
- Yang W, Sun T, Yang Z (2016) Effect of activities associated with coastal reclamation on the macrobenthos community in coastal wetlands of the Yellow River Delta, China: a literature review and systematic assessment. *Ocean Coast Manag* 129:1–9
- Zhang J, Wang J (2000) Combined impacts of MSL rise and the secular trend in MLTR on marine environment in the areas around the Huanghe River mouth. *Mar Sci Bull* 2(1):6–13
- Zhang W, Zhang J, Lin R, Zong H (2013) Tidal response of sea level rise in marginal seas near China. *Adv Water Sci* 24(2):243–250
- Zhang PC, Sun LY, Zhu YL (2015) Reclamation-induced influence on hydrodynamics and suspended sediment concentration at three estuary areas in Bohai Bay. *China Harb Eng* 35(10):6–12
- Zhu L, Wu J, Xu Z, Xu Y, Lin J, Hu R (2014) Coastline movement and change along the Bohai Sea from 1987 to 2012. *J Appl Remote Sens* 8(1):083585

Reproduced with permission of copyright owner. Further reproduction prohibited without permission.